An Overview of Plasmasphere Dynamics I:

Plasmasphere/Magnetosphere Coupling

Jonathan Krall

Retired (formerly of Naval Research Laboratory, Plasma Physics Division)

International School of Space Science

September 26, 2022

Some Credits

NRL Plasma Physics Division	Joseph Huba (now at Syntek) Joel Fedder (now retired)
Also	Joe Borovsky (SWRI) Alex Glocer (NASA/GSFC) Jerry Goldstein (SWRI) Susan Nossal (UWIS) Daniel Weimer (VA Tech) Stan Sazykin (Rice)

Outline

I. What is the plasmasphere?

II. SAMI3 model

III. Dynamics of a plasmasphere plume

IV. Plasmasphere refilling dynamics

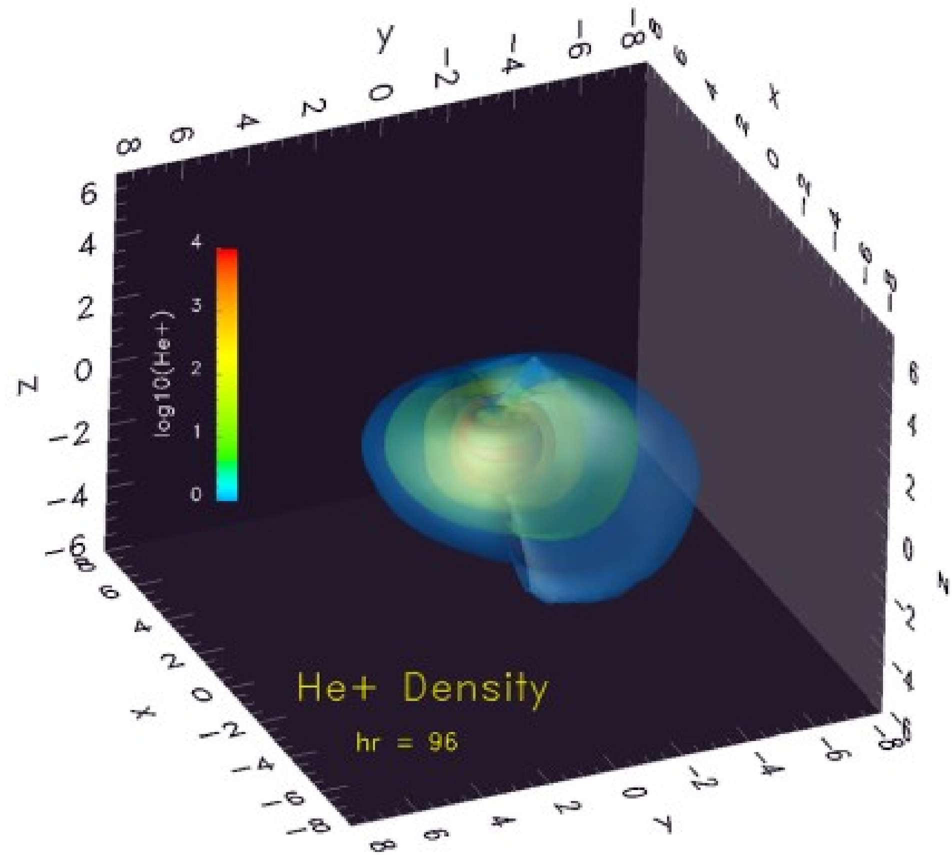

Huba and Krall, GRL, 2013

Throughout, we will look for interesting unsolved problems

I. What is the plasmasphere?

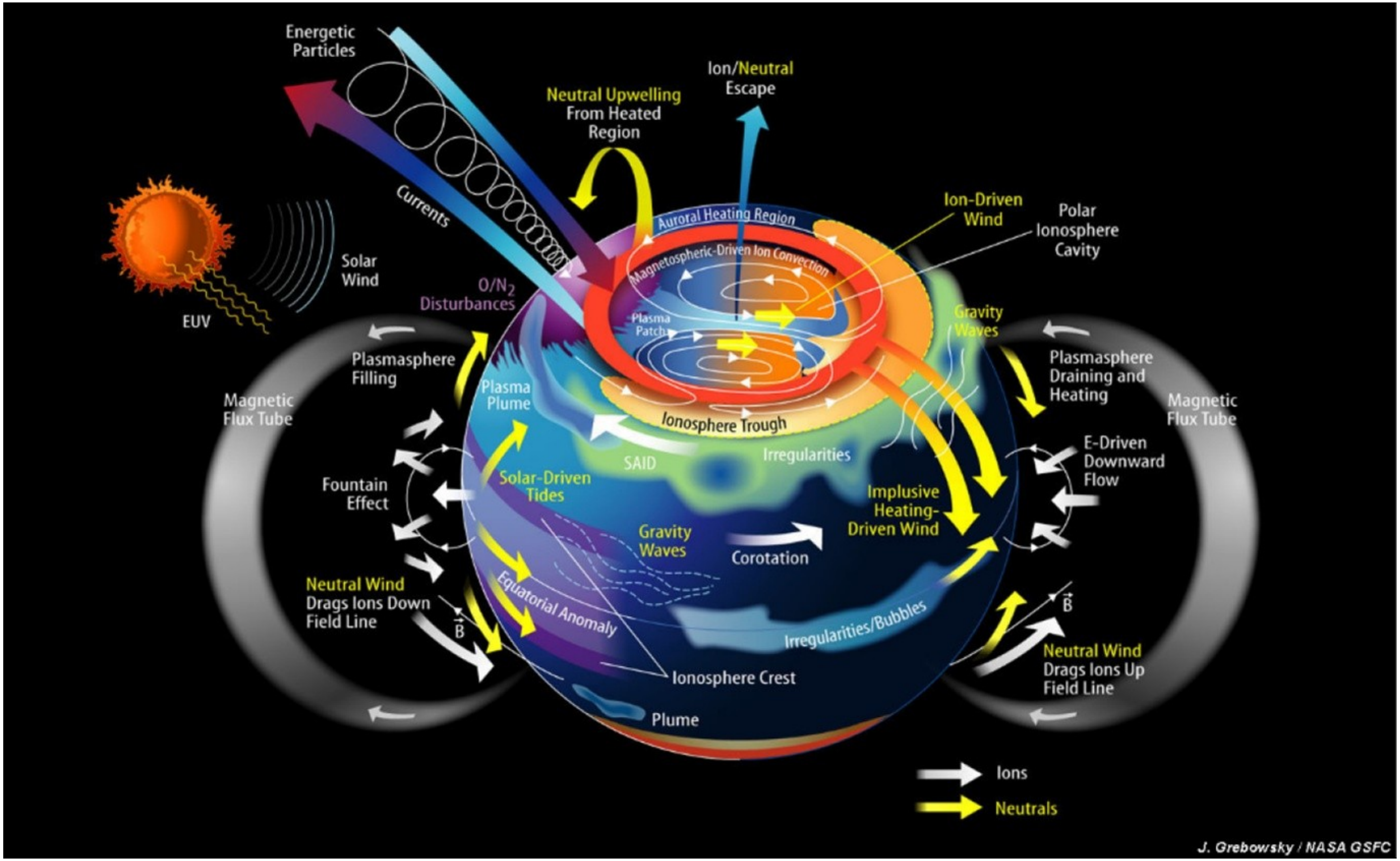

The plasmasphere is like a tail being wagged by two dogs: ionosphere outflow and magnetosphere convection.

Does the plasmasphere matter?

This 2014 advertising photo suggests increasing EM-dependency

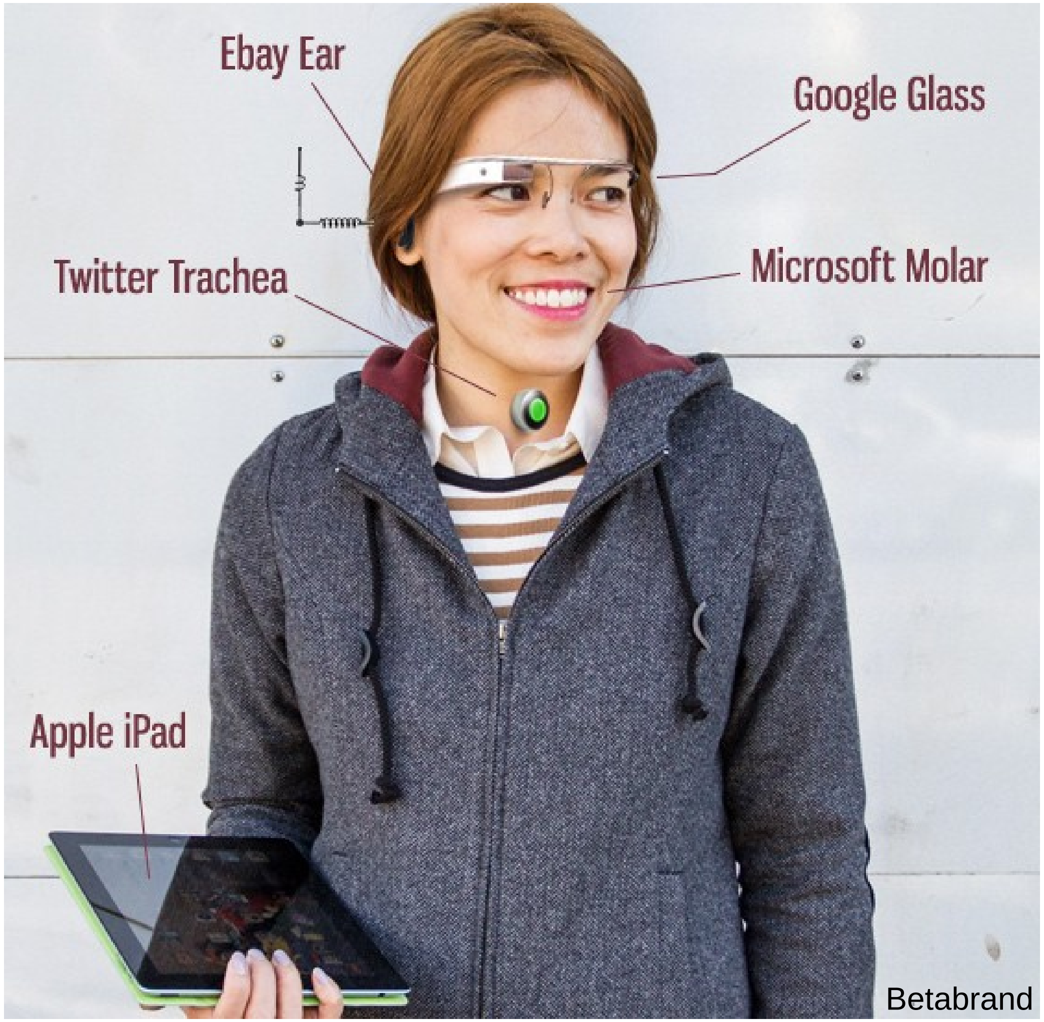

(the actual product is the jacket)

Magnetosphere convection: open and closed field lines

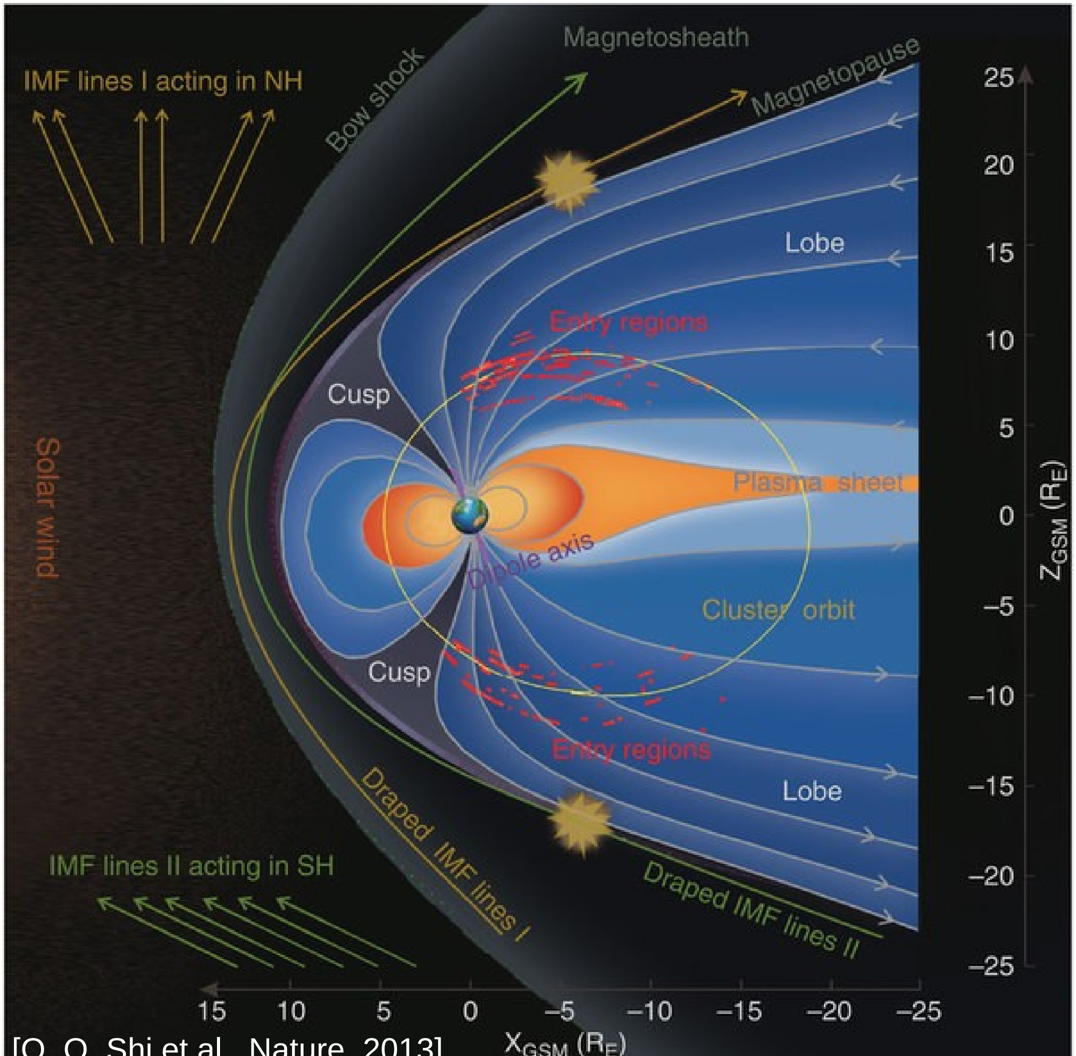

[Q. Q. Shi et al., Nature, 2013]

Geospace is often describes as having ‘open’ and ‘closed’ field lines. Open field lines extend far into space.

Closed field lines can be ‘co-rotating’ (turning with Earth) or convecting from the tail towards the Sun side.

Open field lines convect towards the tail.

Magnetospheric convection shapes the plasmasphere

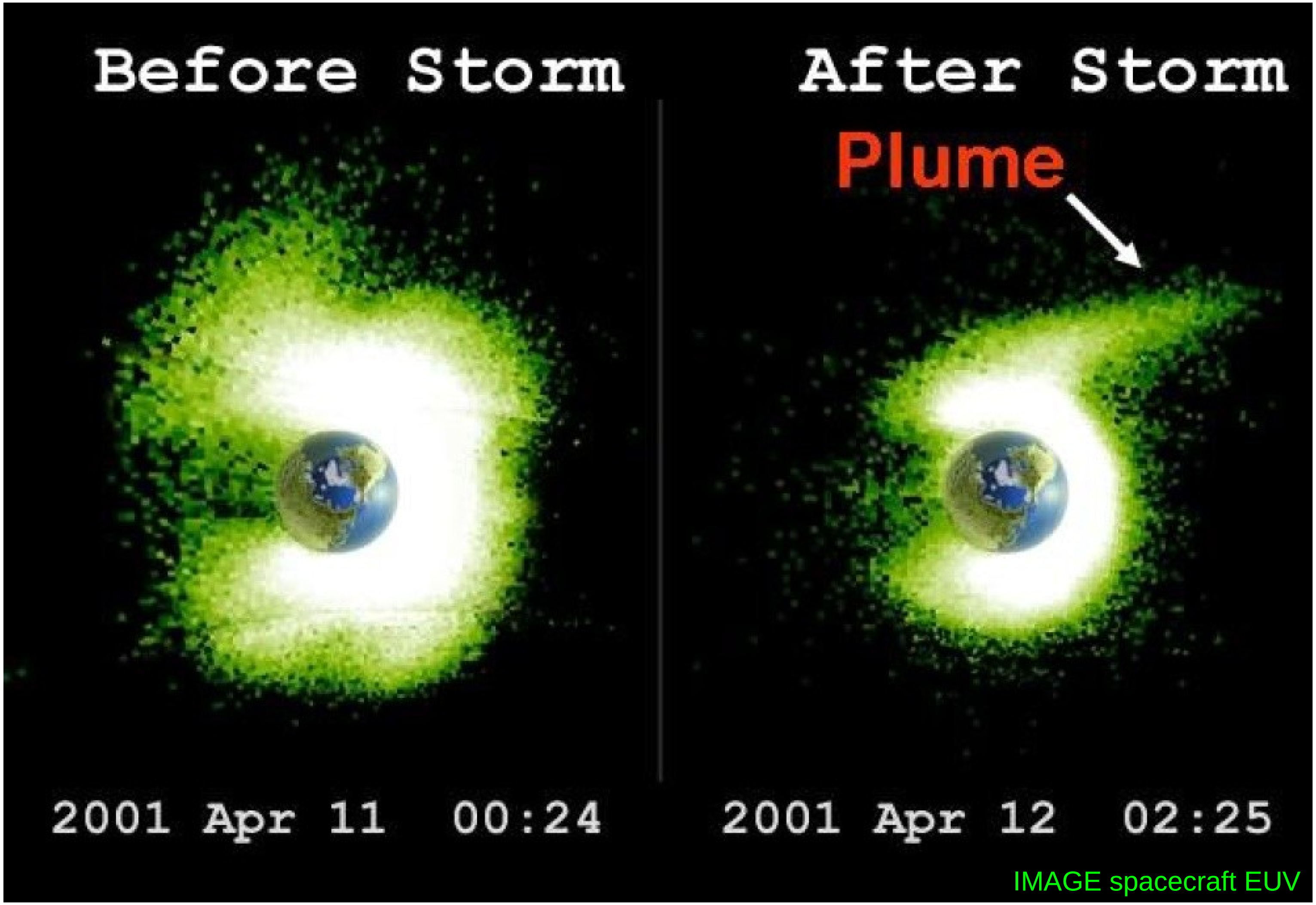

Convection can "carve away" the plasmasphere

Magnetospheric convection

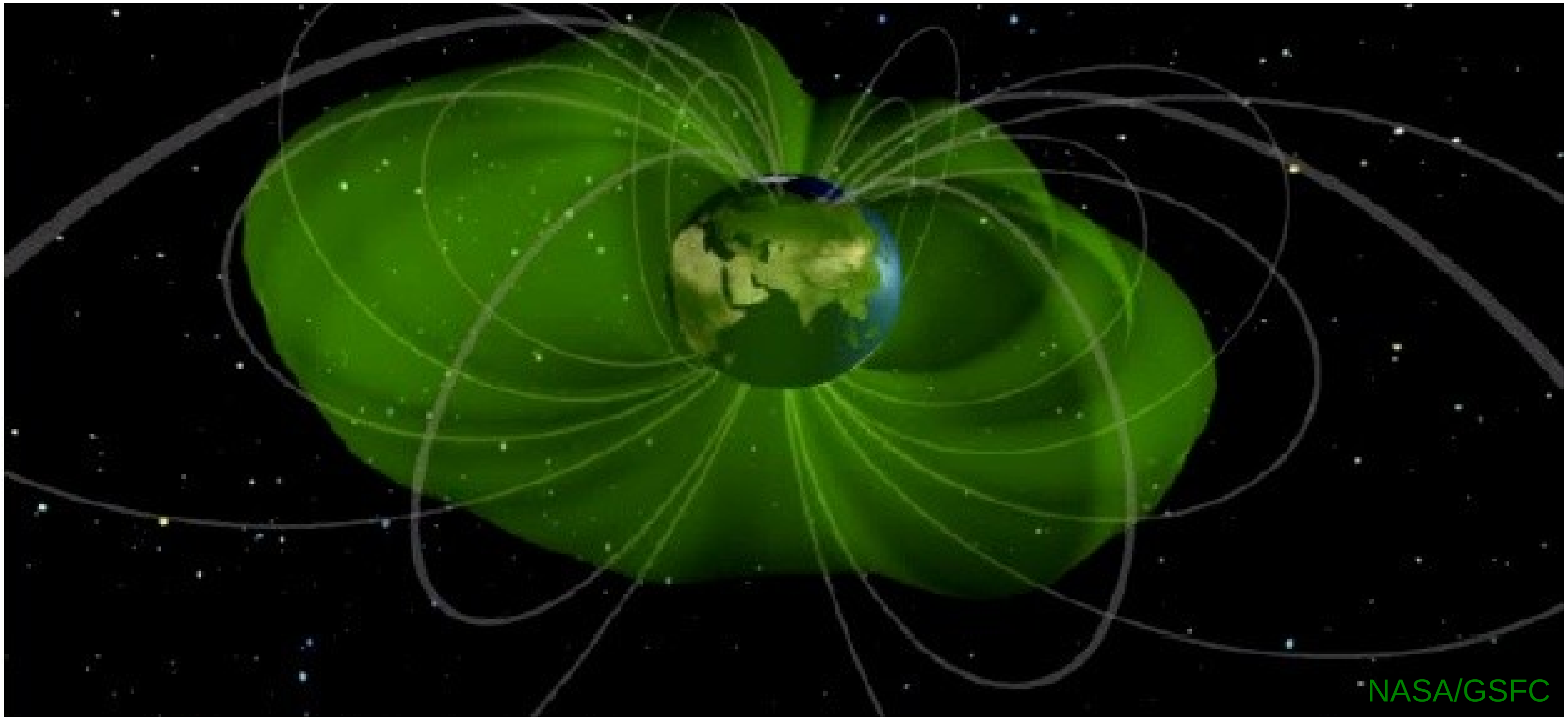

Convection is often described as the movement of field lines.

It can also be described as the **E**×**B** drifts of charged particles.

Either is fine, even though field lines are not physical objects.

ExB drifts

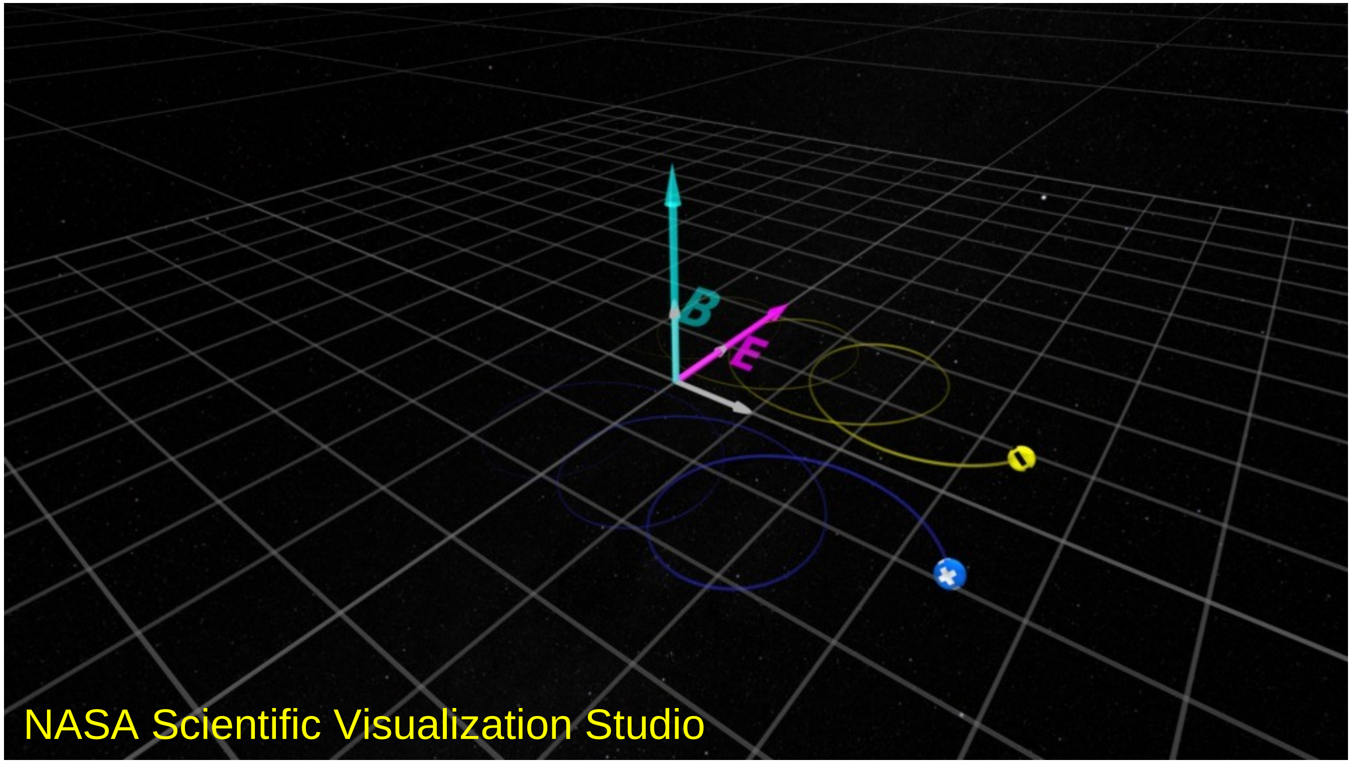

A charged particle in non-parallel E and B fields drifts with a velocity $\mathbf{v} = (\mathbf{E} \times \mathbf{B})/B^2$

Ions and electrons drift together

Magnetospheric convection visualized

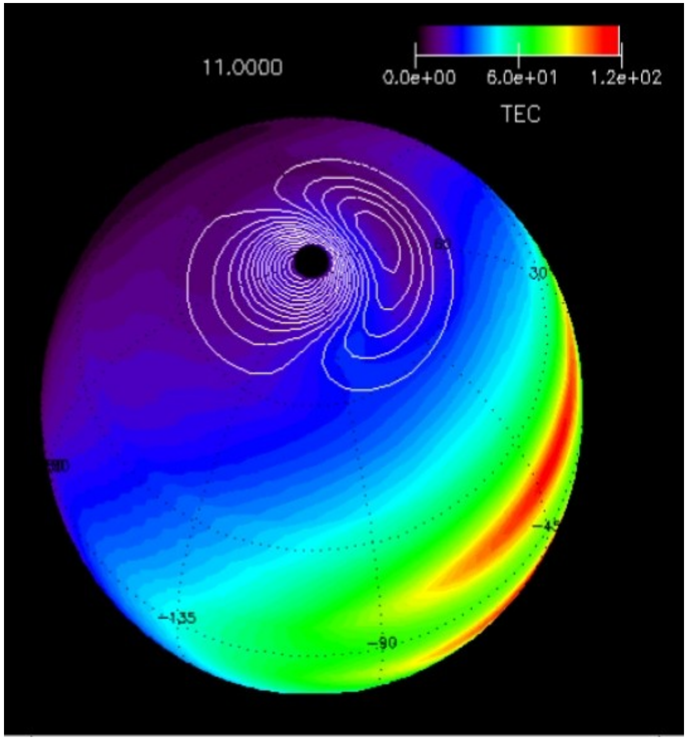

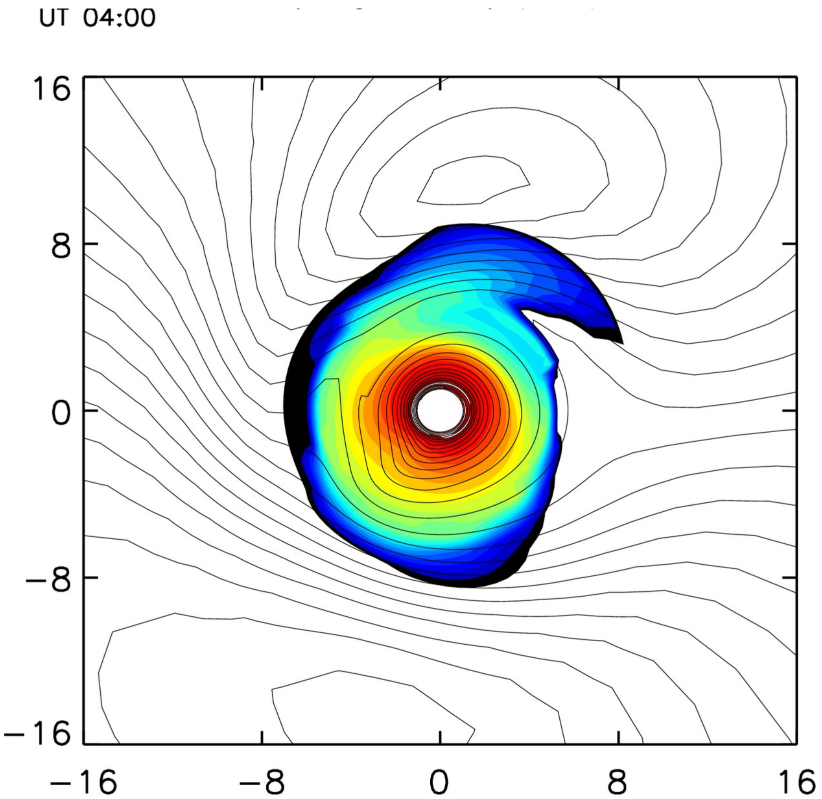

- E x B drifts (or "magnetic field lines") follow potential contours
- Potential contours map along magnetic field lines
- Closed contours near Earth are co-rotating flux tubes
- With a dipole field, mapping is inaccurate at large distances

Magnetospheric convection shapes the plasmasphere

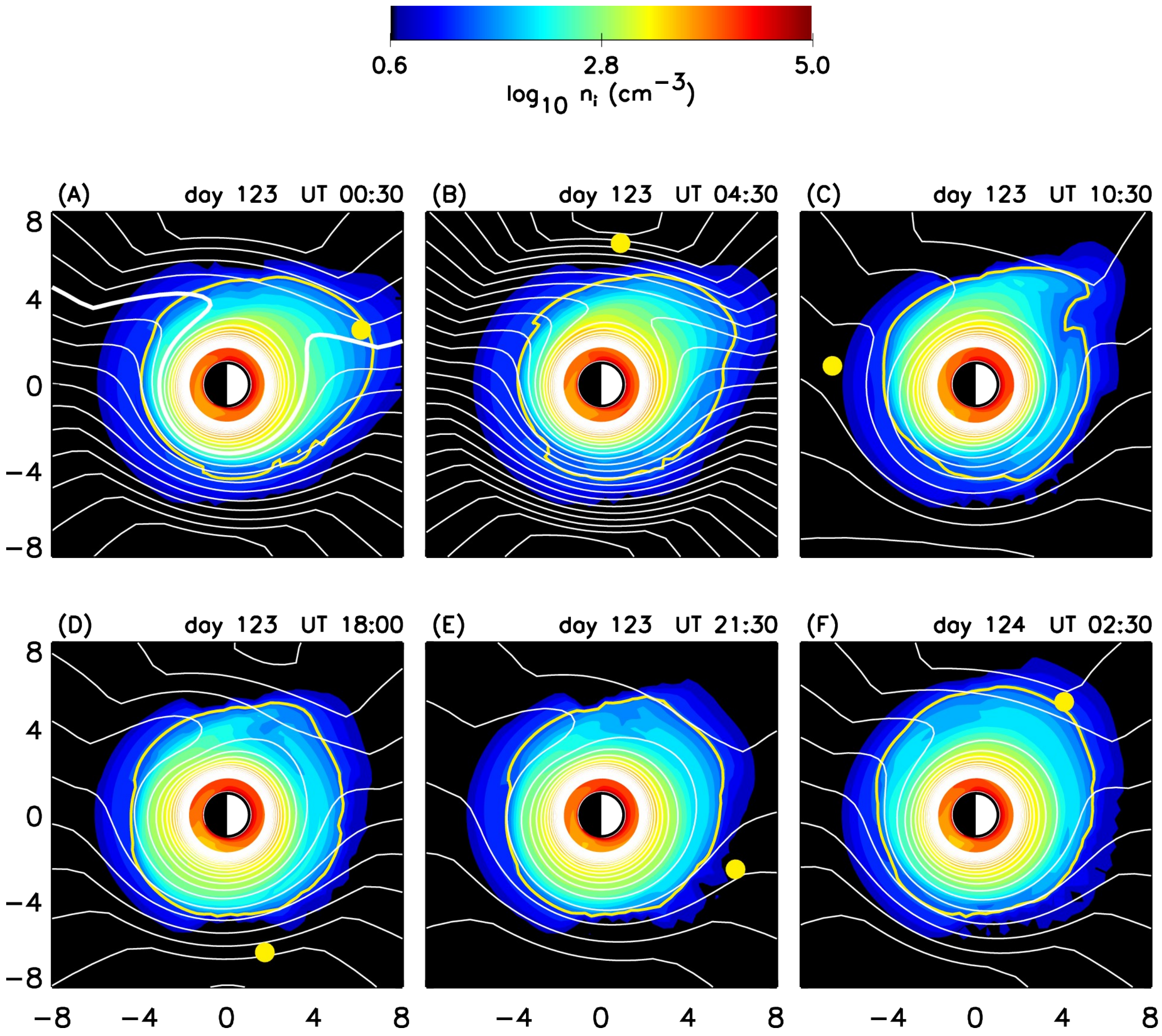

Near-Earth plasmasphere spins with Earth.

The convection is oriented towards the Sun.

Weak convection allows a bigger plasmasphere.

Magnetospheric convection shapes the plasmasphere

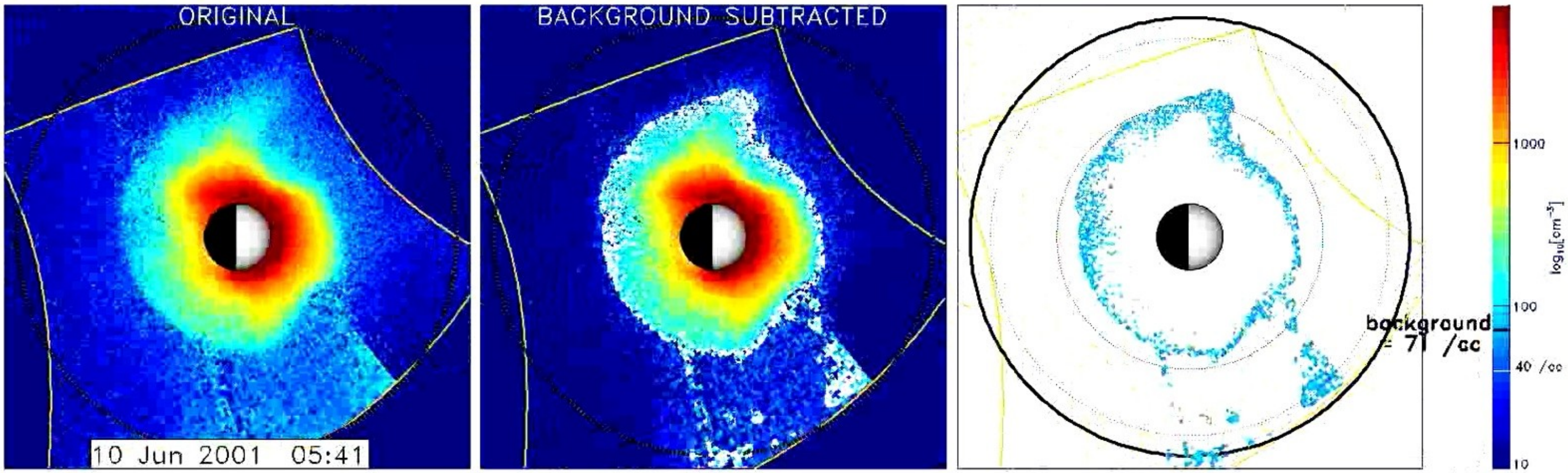

The plasmapause is usually defined as the point on the electron density radial profile with the largest density gradient

IMAGE EUV (Jerry Goldstein)

Magnetospheric convection shapes the ionosphere

Sun ↑

SAMI3/data

2011 DOY 269
September 26

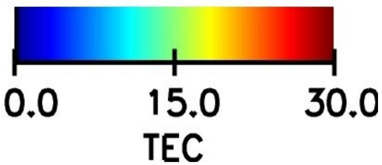

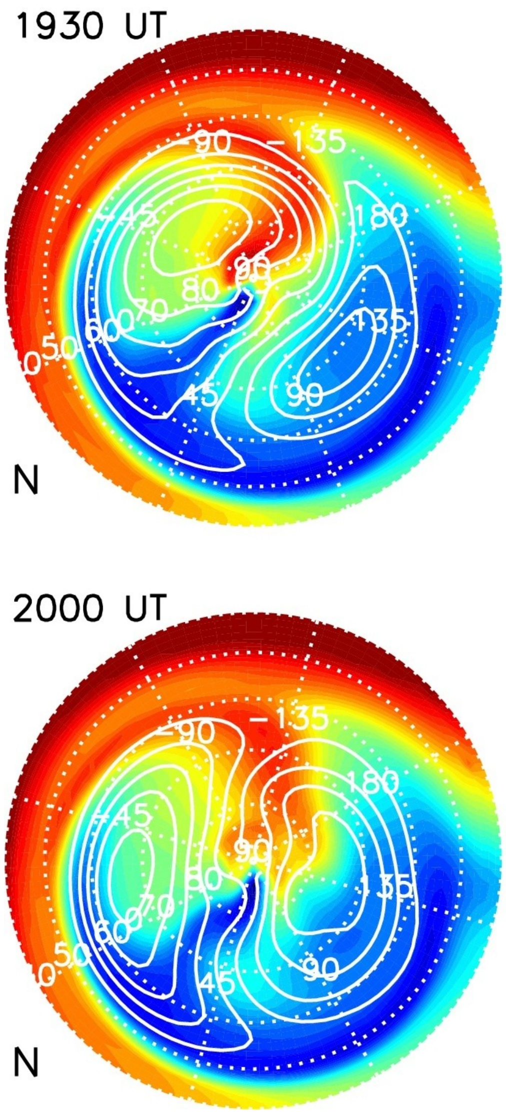

GPS/SuperDARN [Thomas et al., JGR, 2013]

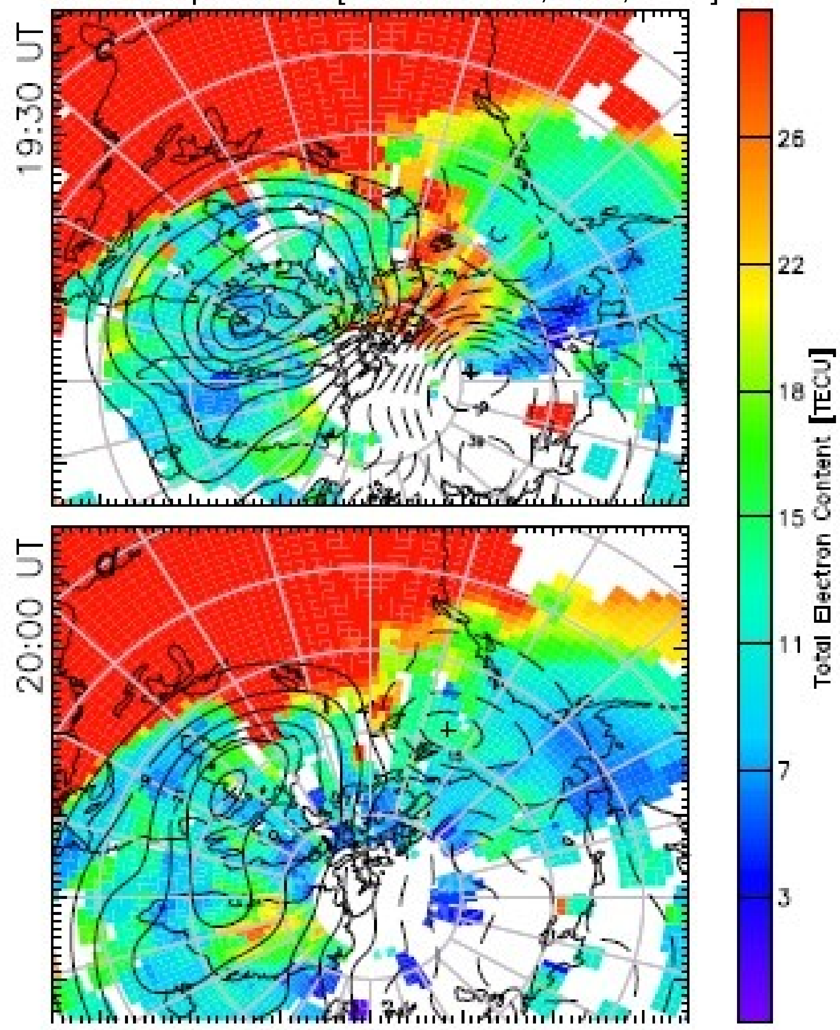

Open and closed field lines

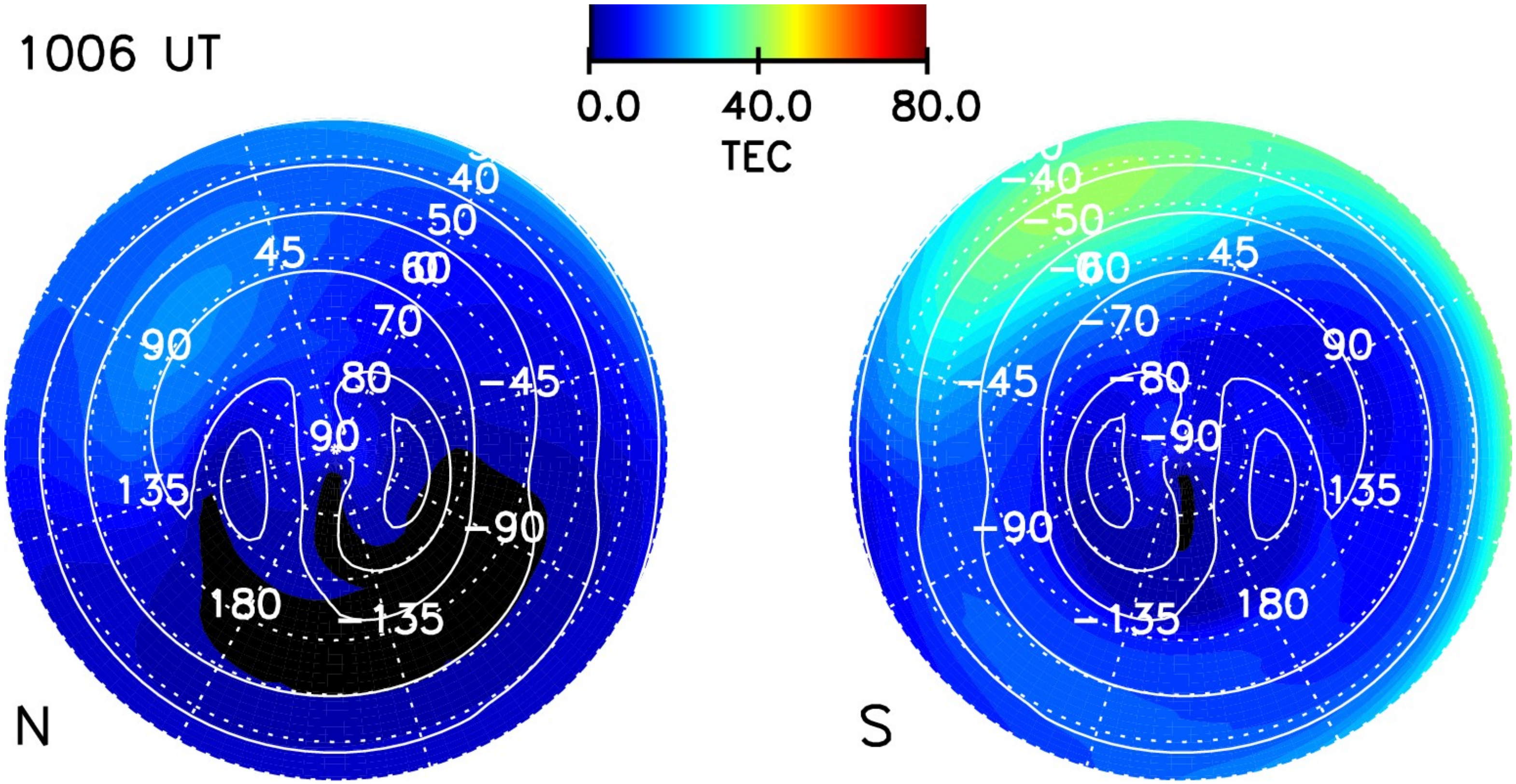

In simulations, northern and southern convection patterns are often quite similar

Open and closed field lines

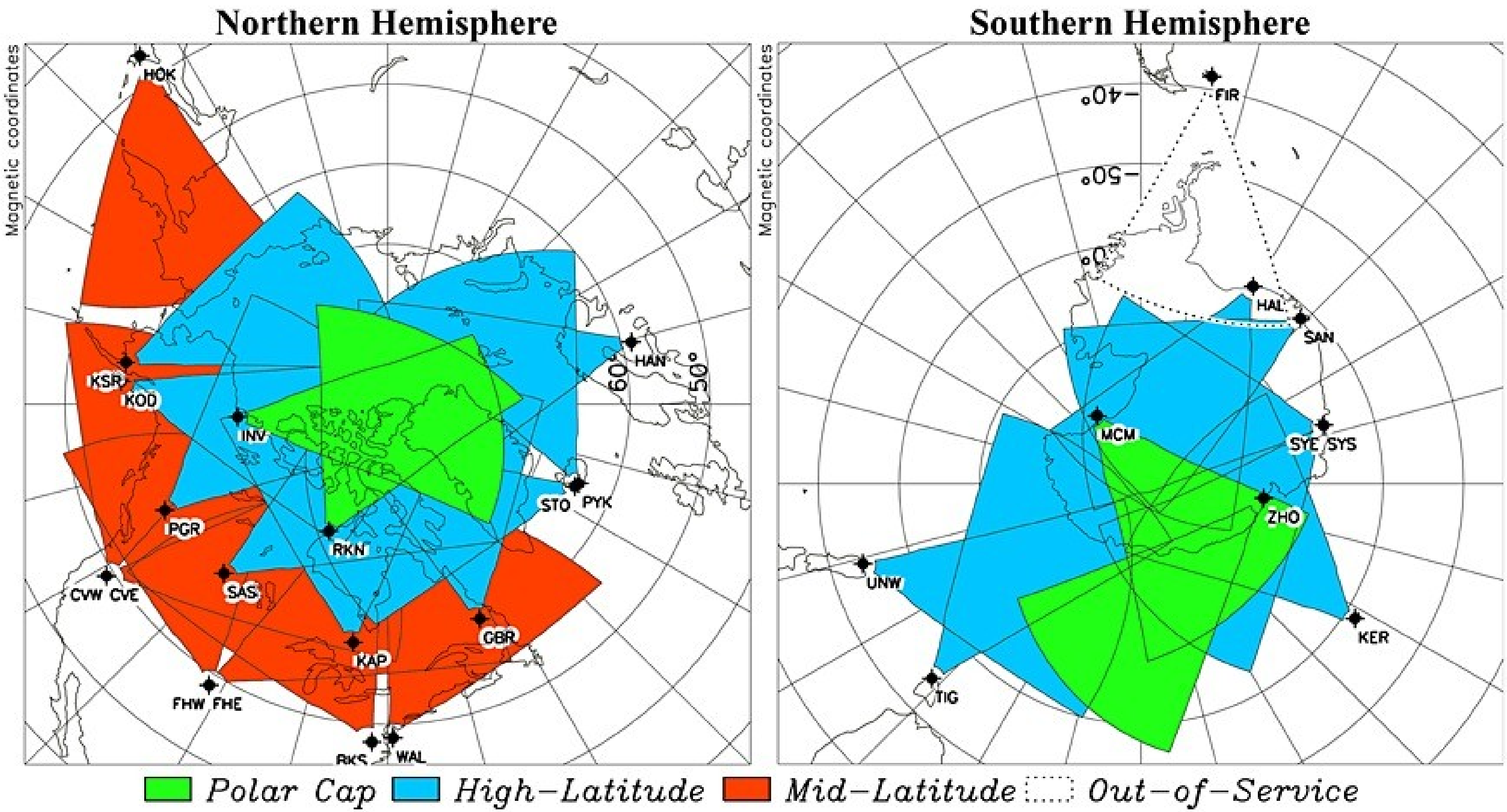

[Thomas et al., JGR, 2013]

Actual northern and southern convection patterns can be measured and might give clues about open and closed convecting field lines

II. SAMI3 model

- Magnetic field: IGRF-like or Non-tilted dipole or Apex model
- Interhemispheric
- Nonorthogonal, nonuniform fixed grid
- Seven (7) ion species (all ions are equal): H^+, He^+, N^+, O^+, N_2^+, NO^+, and O_2^+
  - Solve continuity and momentum for all 7 species
  - Solve temperature for H^+, He^+, O^+, and e^-
- Plasma motion
  - $\mathbf{E} \times \mathbf{B}$ drift perpendicular to $\mathbf{B}$
  - Ion inertia included parallel to $\mathbf{B}$
- Neutral species: NRLMSISE00 and HWM93
- Chemistry: 21 reactions + recombination
- Photoionization: Daytime (EUVAC) and nighttime

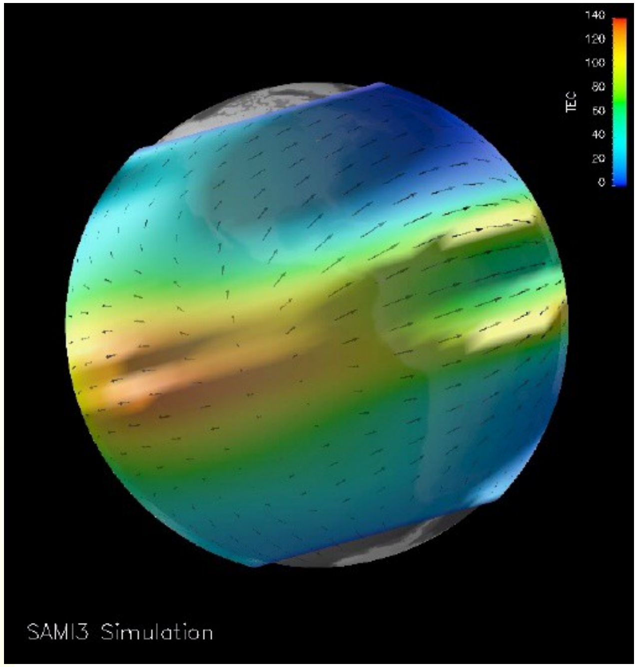

SAMI3 is coupled to a magnetosphere potential model and a thermosphere model.

[Huba et al., JGR, 2000; Huba and Krall, GRL, 2013]

NRL SAMI3 Ionosphere/Plasmasphere Model

- ion continuity

$$\frac{\partial n_i}{\partial t} + \nabla \cdot (n_i \mathbf{V}_i) = P_i - L_i n_i$$

- ion velocity

$$\frac{\partial \mathbf{V}_i}{\partial t} + \mathbf{V}_i \cdot \nabla \mathbf{V}_i = -\frac{1}{\rho_i}\nabla \mathbf{P}_i + \frac{e}{m_i}\mathbf{E} + \frac{e}{m_i c}\mathbf{V}_i \times \mathbf{B} + \mathbf{g}$$

$$-\nu_{in}(\mathbf{V}_i - \mathbf{V_n}) - \sum_j \nu_{ij}\left(\mathbf{V}_i - \mathbf{V}_j\right)$$

- ion temperature

$$\frac{\partial T_i}{\partial t} + \mathbf{V}_i \cdot \nabla T_i + \frac{2}{3} T_i \nabla \cdot \mathbf{V}_i + \frac{2}{3}\frac{1}{n_i k}\nabla \cdot \mathbf{Q}_i = Q_{in} + Q_{ij} + Q_{ie}$$

[Huba et al., JGR, 2000]

NRL SAMI3 Ionosphere/Plasmasphere Model

$$\nabla \cdot \Sigma \nabla \Phi = S(g, V_n, J_{\|}) \qquad \mathbf{E} = -\nabla \Phi$$

$$\underbrace{\frac{\partial}{\partial p}\Sigma_{pp}\frac{\partial \Phi}{\partial p} + \frac{\partial}{\partial \phi}\Sigma_{p\phi}\frac{\partial \Phi}{\partial \phi}}_{\text{Pedersen}} \underbrace{- \frac{\partial}{\partial \phi}\Sigma_{H}\frac{\partial \Phi}{\partial p} + \frac{\partial}{\partial p}\Sigma_{H}\frac{\partial \Phi}{\partial \phi}}_{\text{Hall}} =$$

$$\underbrace{-\frac{1}{2}\frac{\partial F_{pV}}{\partial p} + \frac{1}{2}\frac{\partial F_{pg}}{\partial p} + \frac{\partial F_{\phi V}}{\partial \phi} + \frac{\partial F_{\phi g}}{\partial \phi}}_{\text{neutral wind and gravity}}$$

Typically the wind-driven dynamo potential is computed and the solar-wind-driven magnetospheric potential is added.
Models also coupled through conductance, density, etc.

Typically: 96 longitudes, 120 “field lines”, 300 points per field line

SAMI3: The NRL Ionosphere/Plasmasphere Model

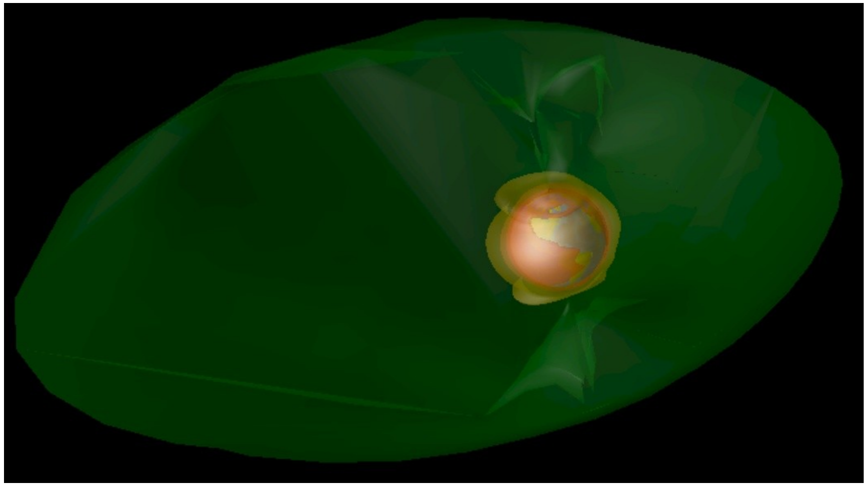

The SAMI3 grid extends out into space to beyond 8 Re

SAMI3 includes zonal **E**x**B** drifts

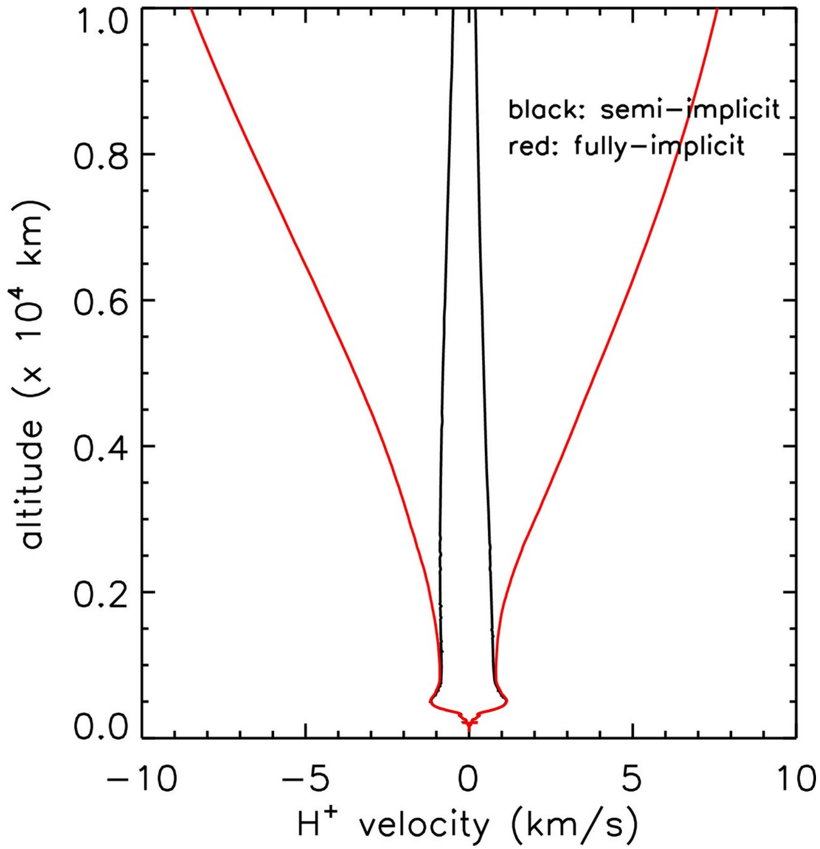

SAMI3 does not use the diffusive approximation, which is valid at low altitudes (below 1000 km)

[Huba et al. JGR (2000, 2017); Huba & Joyce AGU monograph v201 (2014)]

Geospace modeling

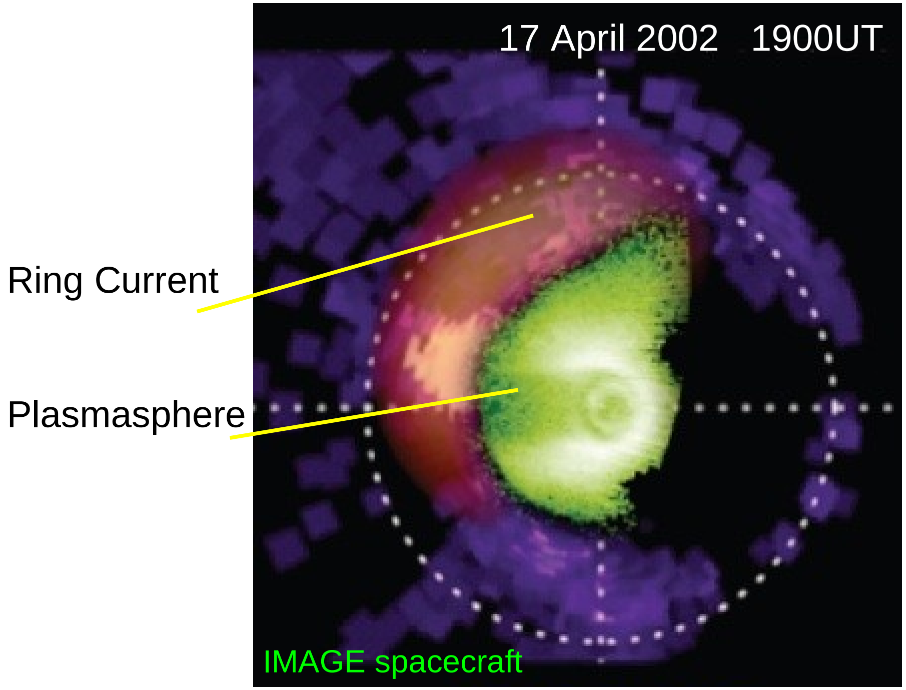

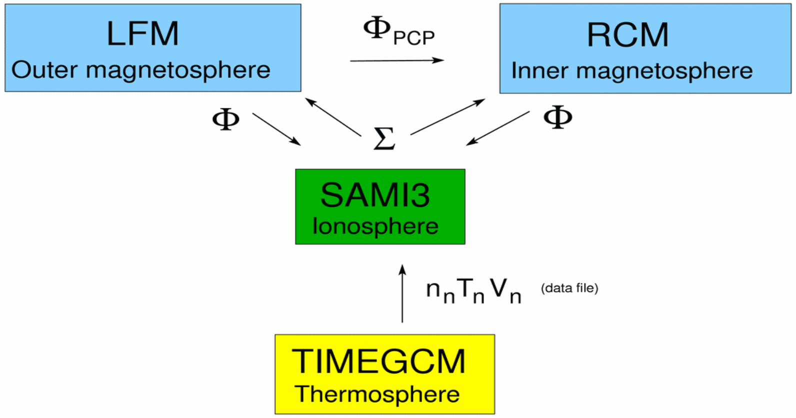

We have all the pieces, and have been coupling them together in various ways.

We can also use empirical models.

III. Dynamics of a Plasmasphere Plume

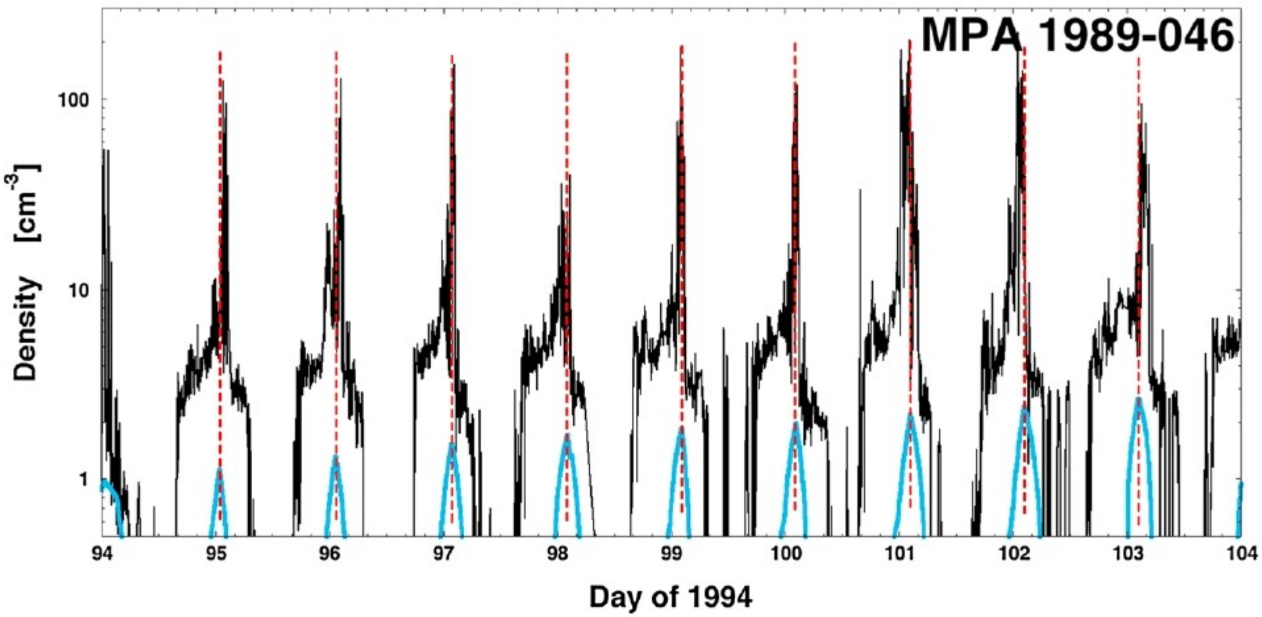

Figure 15. During the long-lived storm of April 1994, the number density of the long-lived drainage plume as measured by the spacecraft 1989–046 is plotted for nine crossing of the plume (black). For a computer simulation of the April 1994 storm using the DGCPM code, the simulated number density of plasmaspheric plasma at the location of 1989–046 is plotted in blue.

In two examples of long-lived storms (> 10 days), a plume was observed from a geosynchronous orbit throughout the storm. An empirical plasmasphere code did not reproduce the result.

[Borovsky et al., JGR, 2014]

The plume and the tongue of ionization

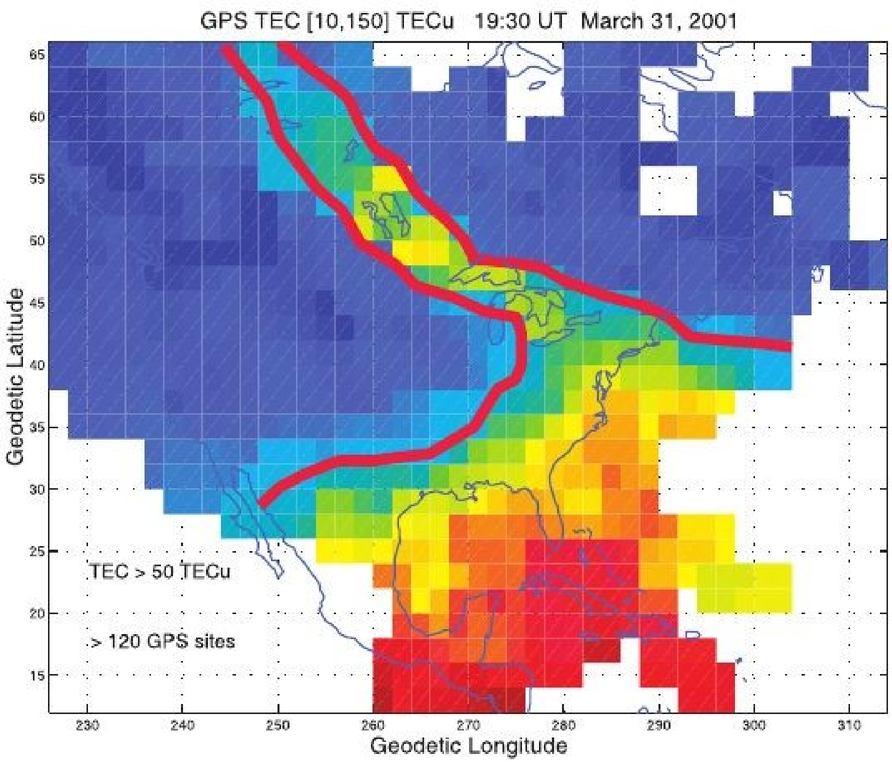

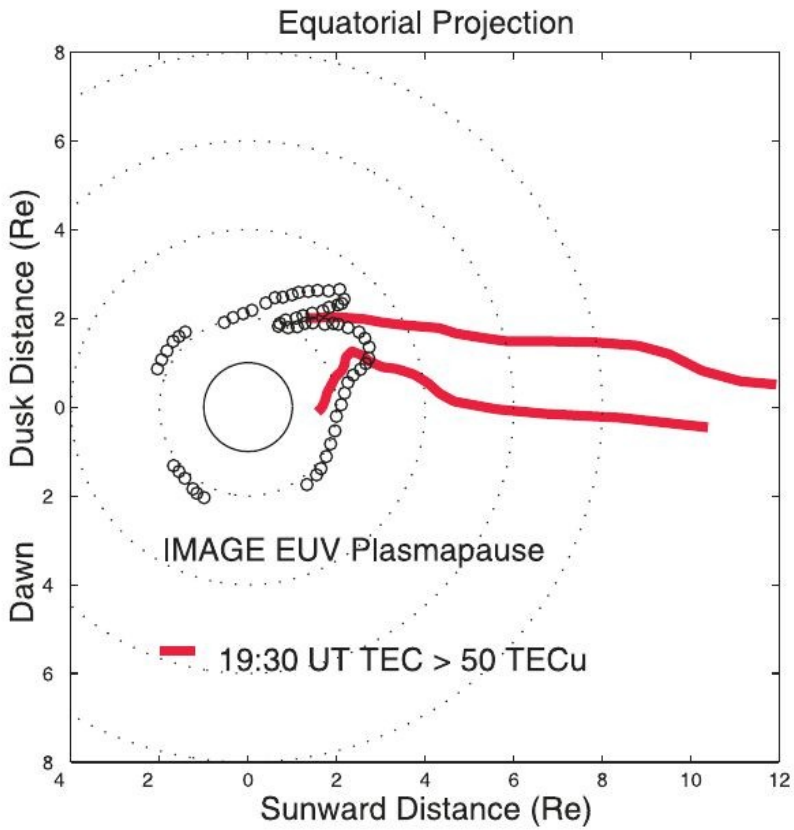

The connection between the plume and the tongue of ionization have been observed, but not in detail.

[Foster et al, GRL, 2002]

SAMI3 simulation a plasmasphere plume

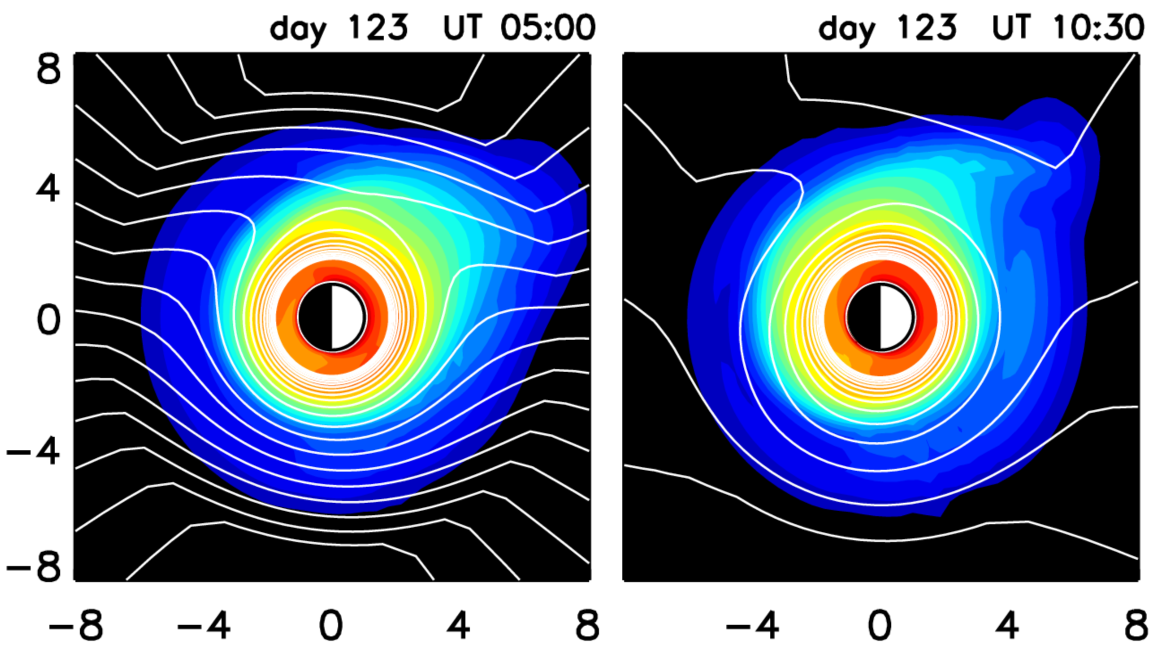

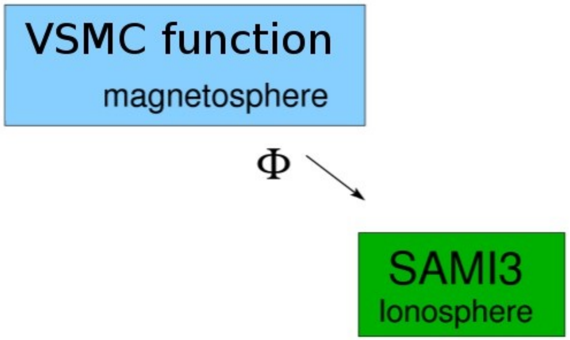

$$\Phi = Ar^2 \sin\phi$$

$$A = \frac{0.045}{(1 - 0.159K_p + 0.0093K_p^2)^3}\ [\mathrm{kV}/R_E^2]$$

Plume sharpens when potential weakens.

[Reinisch et al., 2009, Space Sci. Rev.]

[Krall et al., GRL, 2018]

SAMI3 simulation a plasmasphere plume

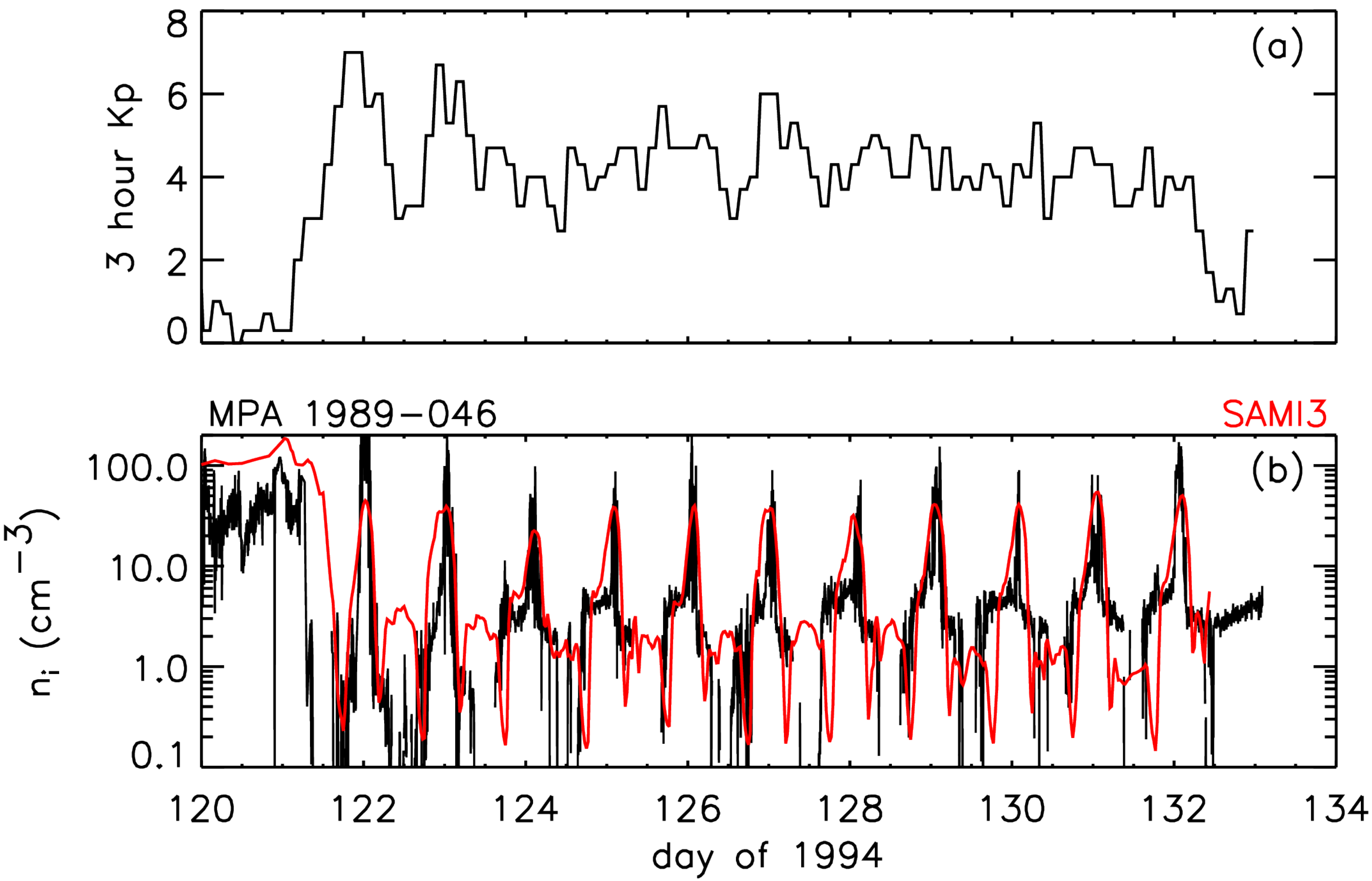

Why does it work? Where does the plume plasma come from?

What is a plume?

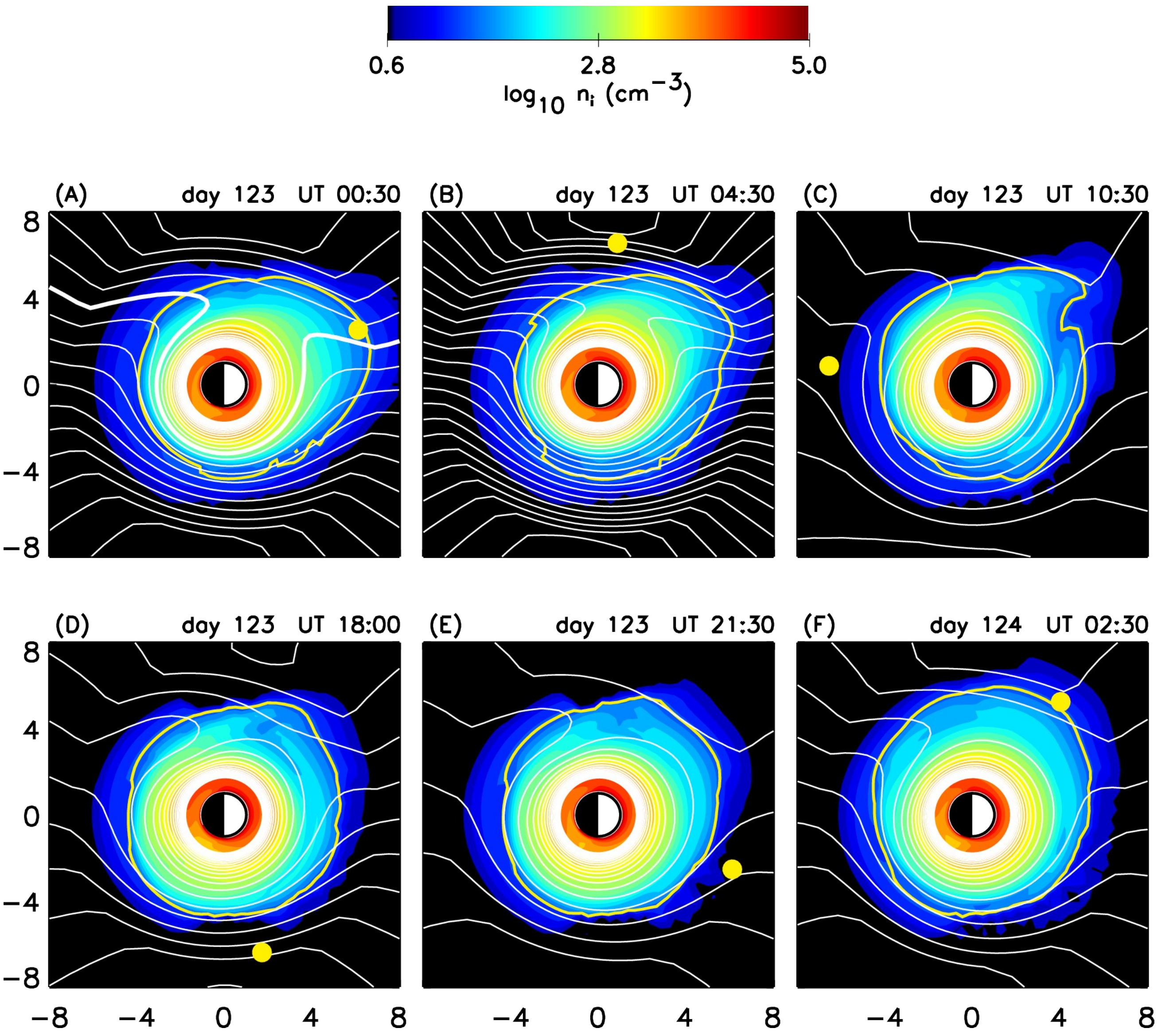

The spacecraft finds a plume on every pass.

The ‘plume’ is present whether it looks like a plume or not.

It is considered a plume because the density is high.

Good agreement from peak to peak

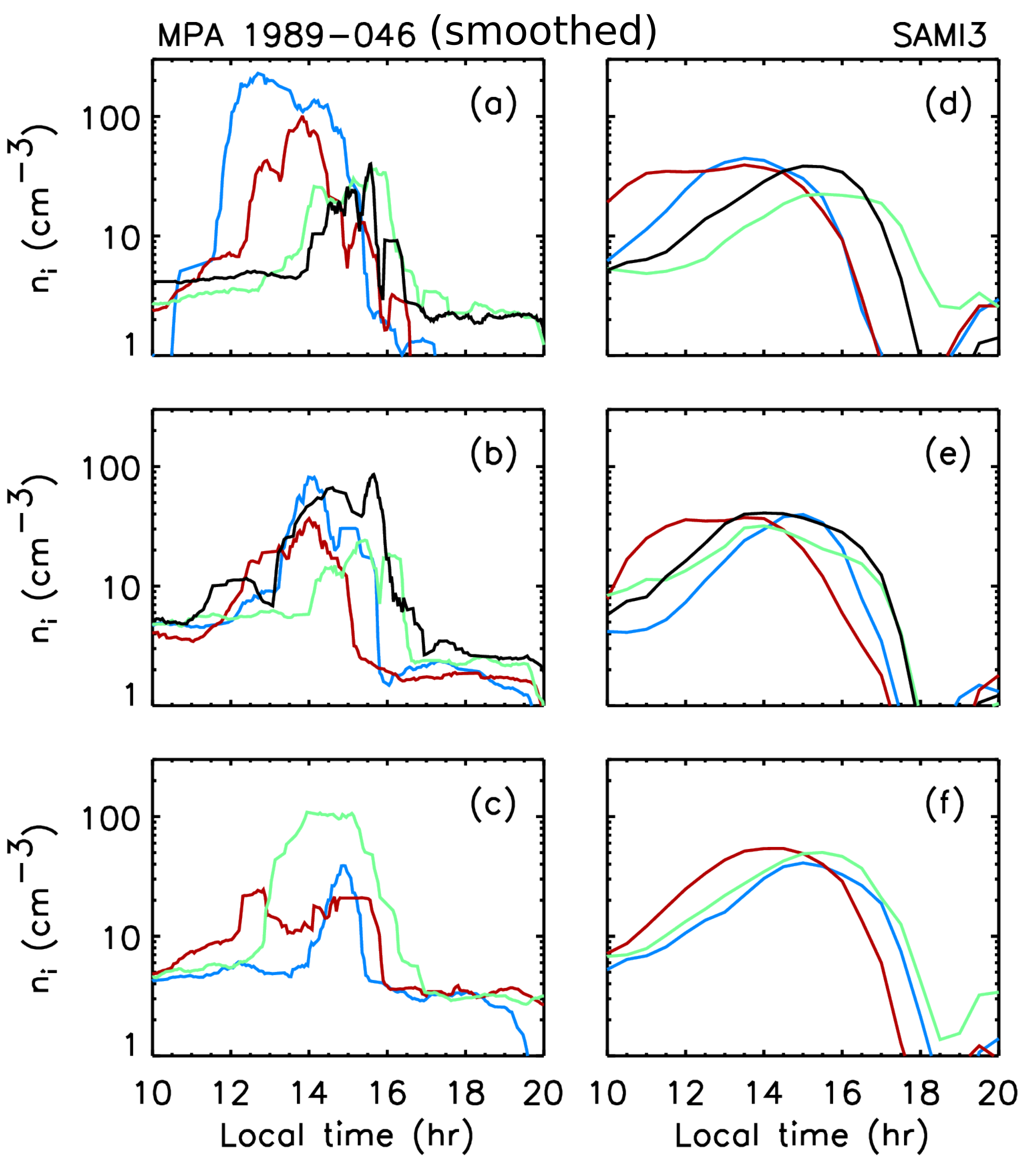

The VSMC potential captures the shifting plume position to some degree.

The pre-peak density (2-6 cm^{-3}) and the post-peak density (1-3 cm^{-3}) indicate background density.

High-speed outflows feed the plume

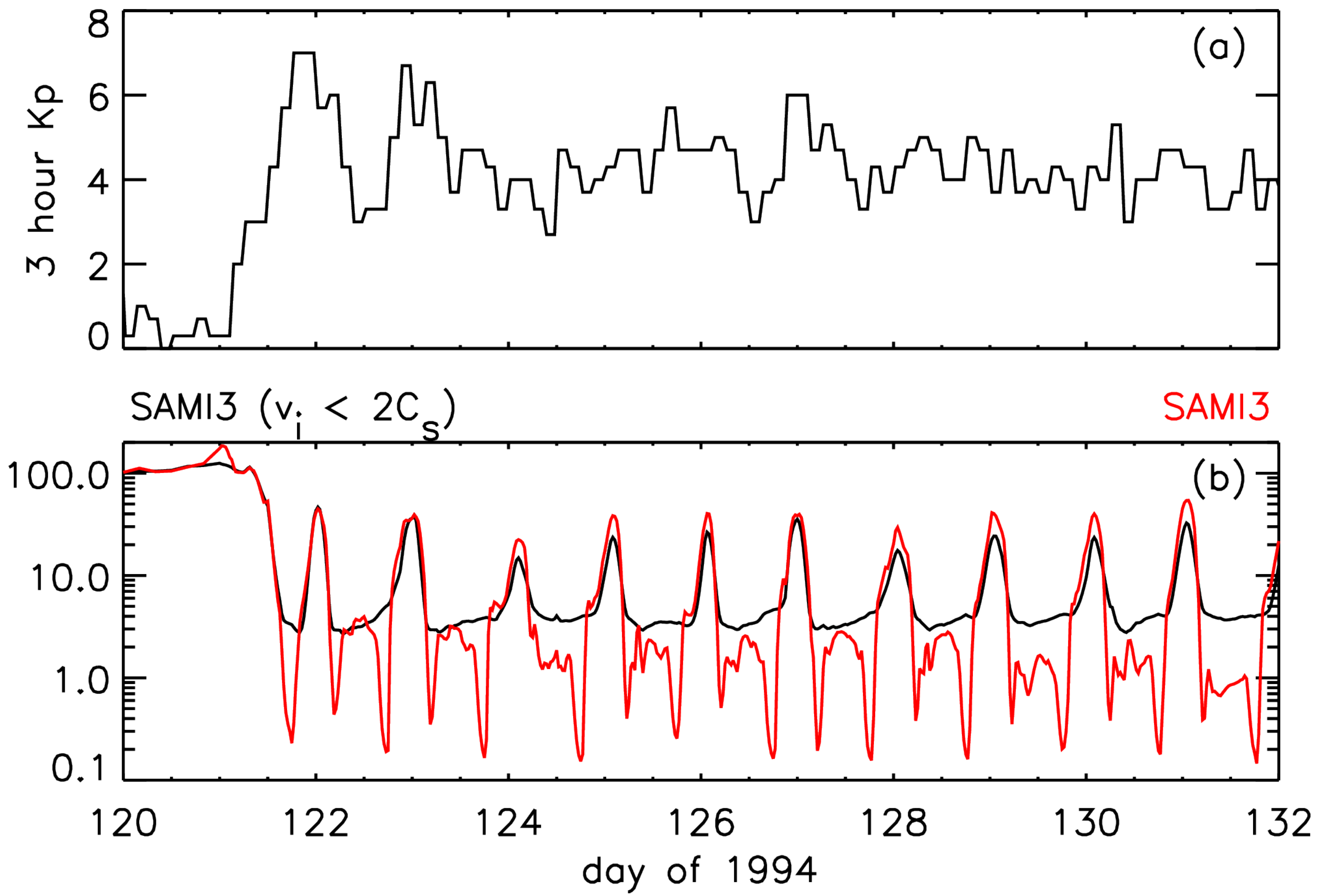

Where does the density come from?

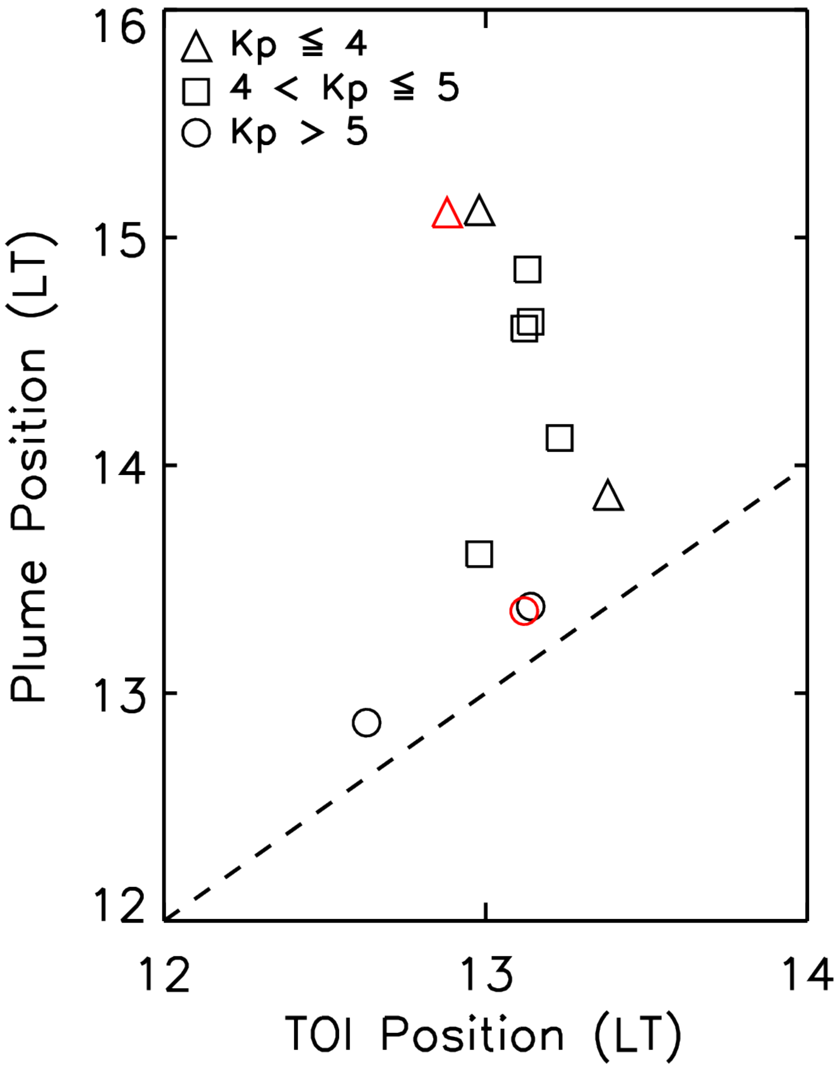

A plume is always present in the sense that the density vs. local time has a peak in the afternoon sector. The “tongue of ionization” is similarly always present

The correlation between the TOI position and the plume is strongest when Kp is high.

IV. Plasmasphere refilling dynamics

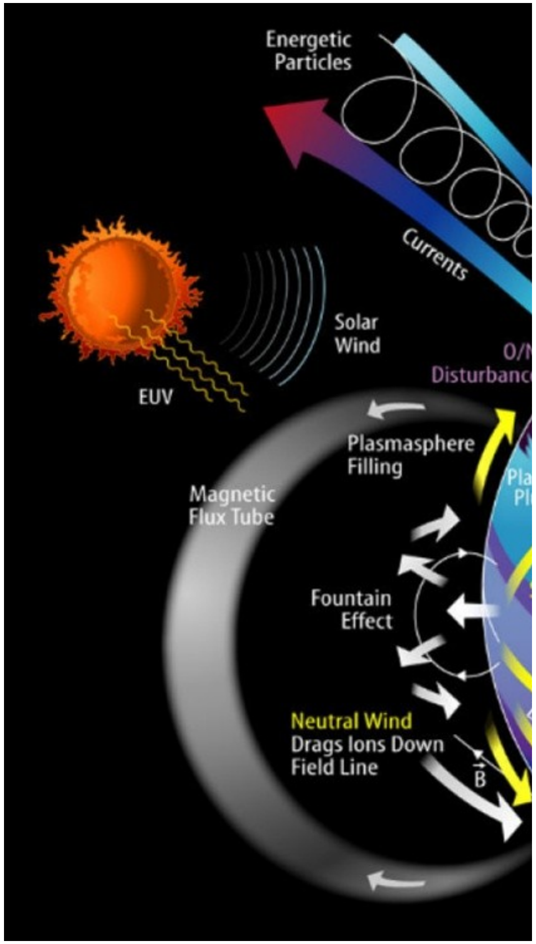

[Denton et al., 2012]

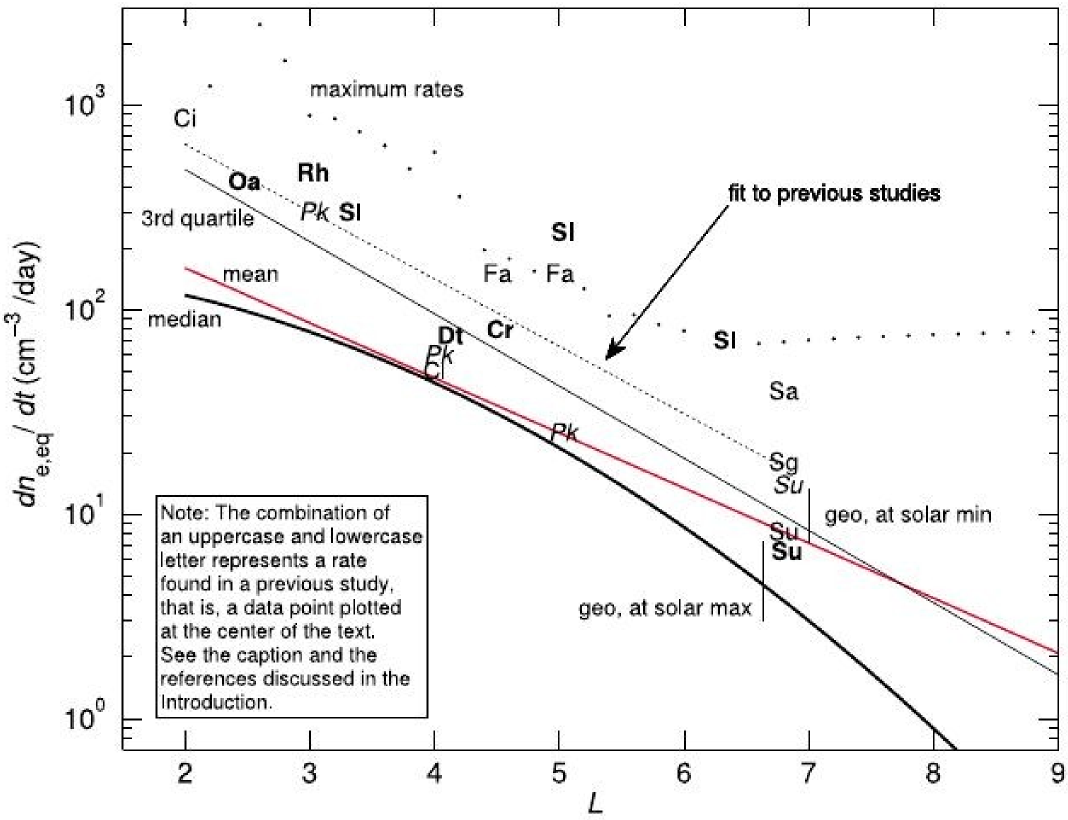

Refilling rates from IMAGE database (red and black curves) are lower than in past studies.

Plasmasphere refilling dynamics: what is refilling?

[Obana et al., 2010]

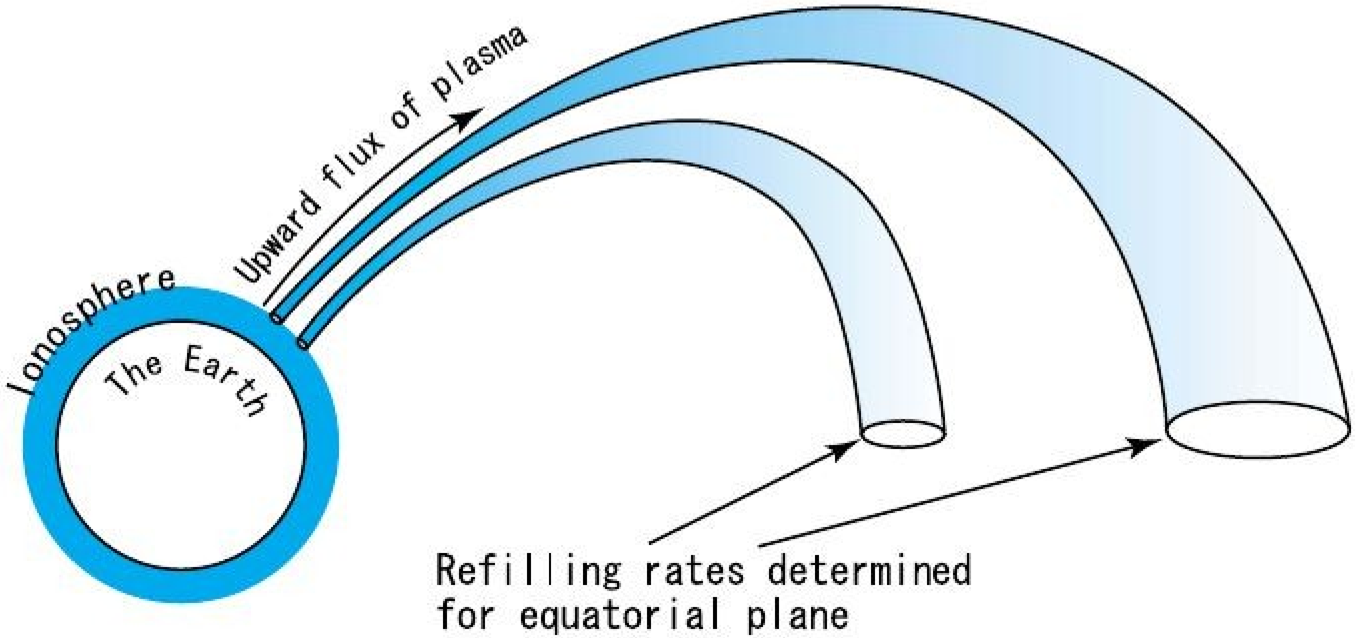

The refilling rate is the change in the equatorial number density.
This can be a global average or the density in a reference flux tube.

In many respects, plasmasphere refilling is not well-understood.

Refilling dynamics vary with the solar cycle

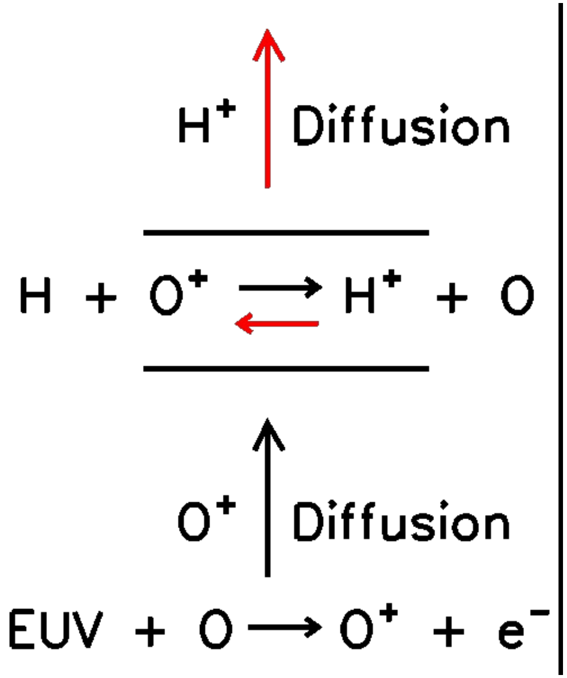

[Rasmussen et al., PlanetSpaceSci, 1993]

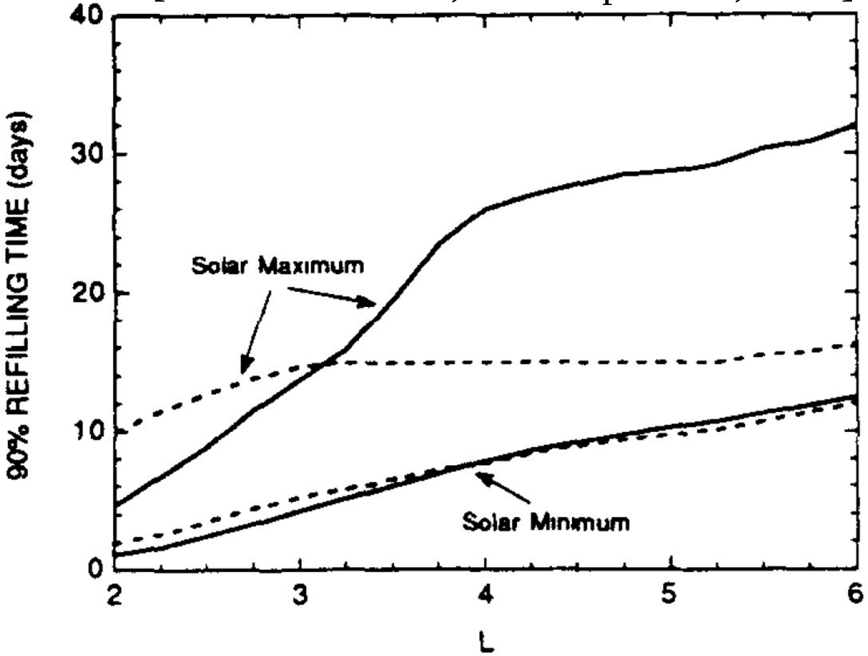

Refilling is affected by H supply, O^+ supply and O^+, H^+ transport. Refilling is slower at solar max because H supply is much lower and because O^+ transport (O-O^+ collisions) is slower.

The H density in the thermosphere and exosphere is of interest.

Refilling is affected by the exosphere H density

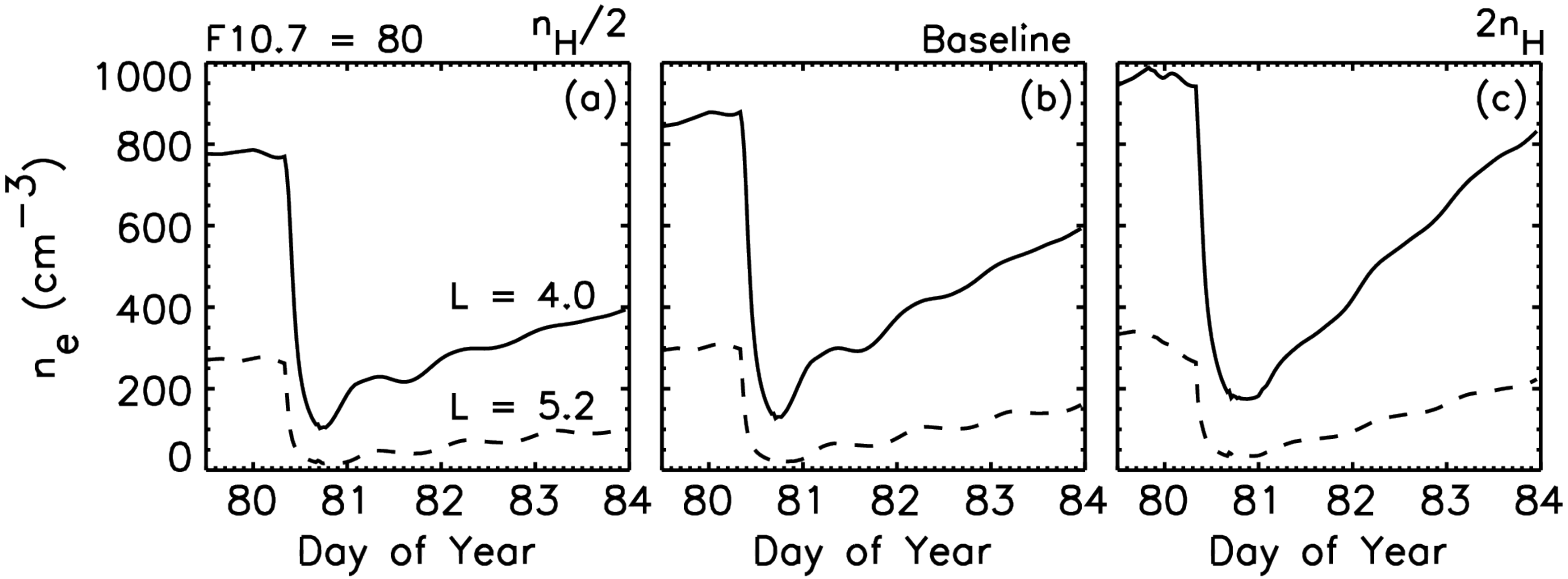

- Refilling rate varies nearly linearly with H density
- Nossal et al. JGR (2016): H varies with climate
- We need better models of exospheric H and O

[Krall et al., Space Weather, 2018]

Refilling is affected by the neutral H density

[Krall et al., Space Weather, 2018]

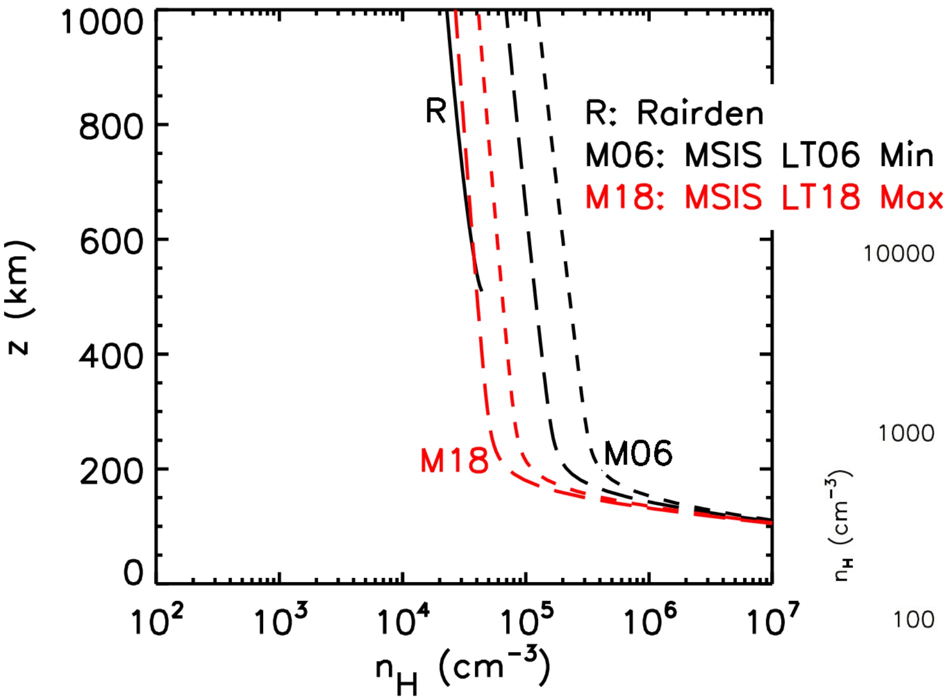

[Illie et al., JASTP, 2013]

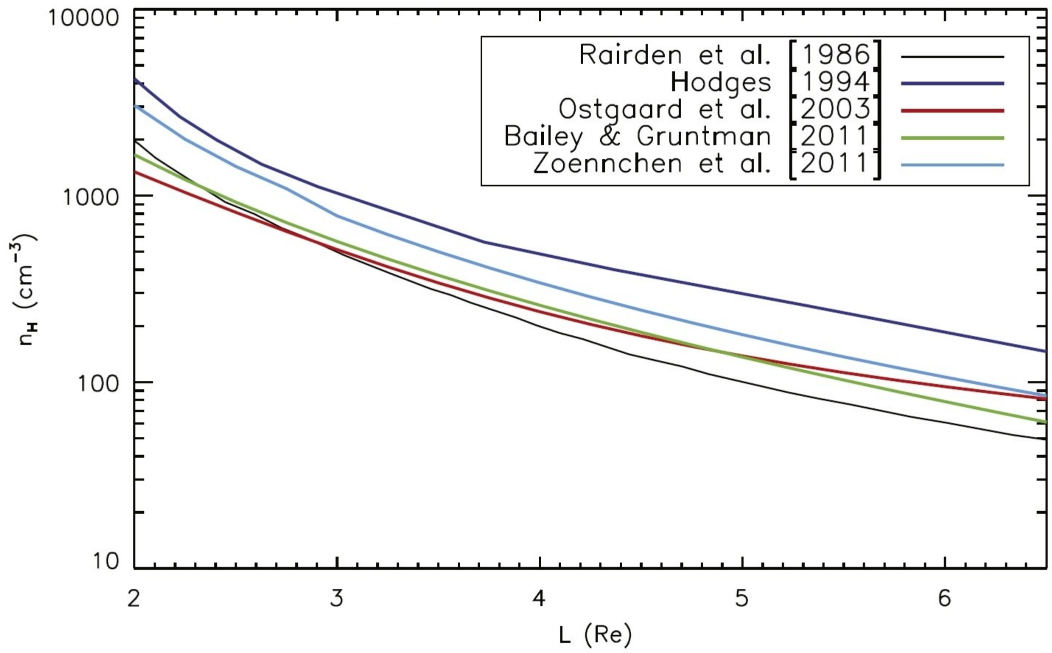

Bishop [Plan. Space Sci. 1991]: exosphere can be described in terms of ballistic, escaping, and orbiting particle populations

Early-stage and late-stage plasmasphere refilling

[Lawrence et al., JGR, 1999]

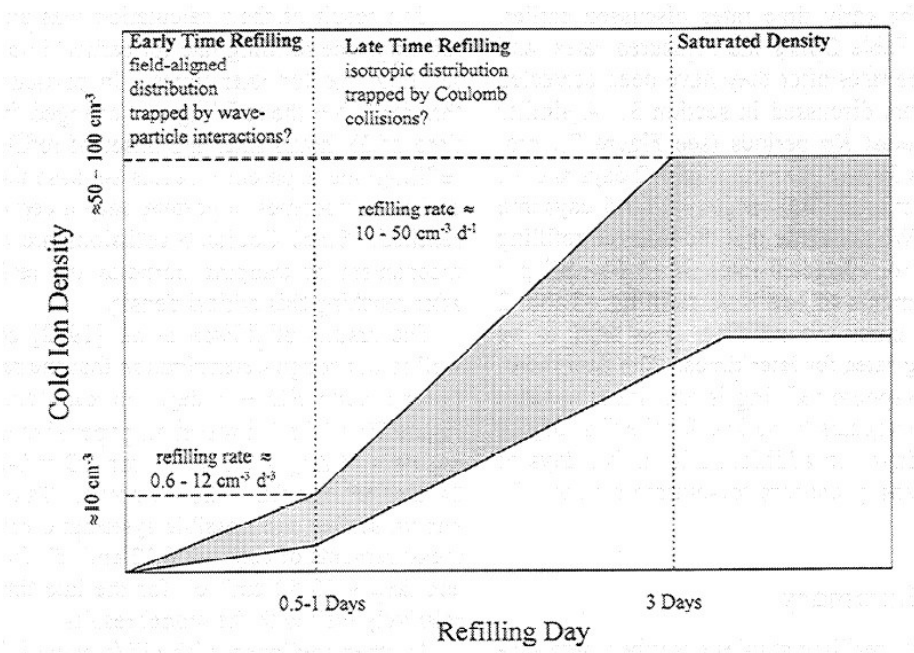

[Krall & Huba, GRL, 2019]

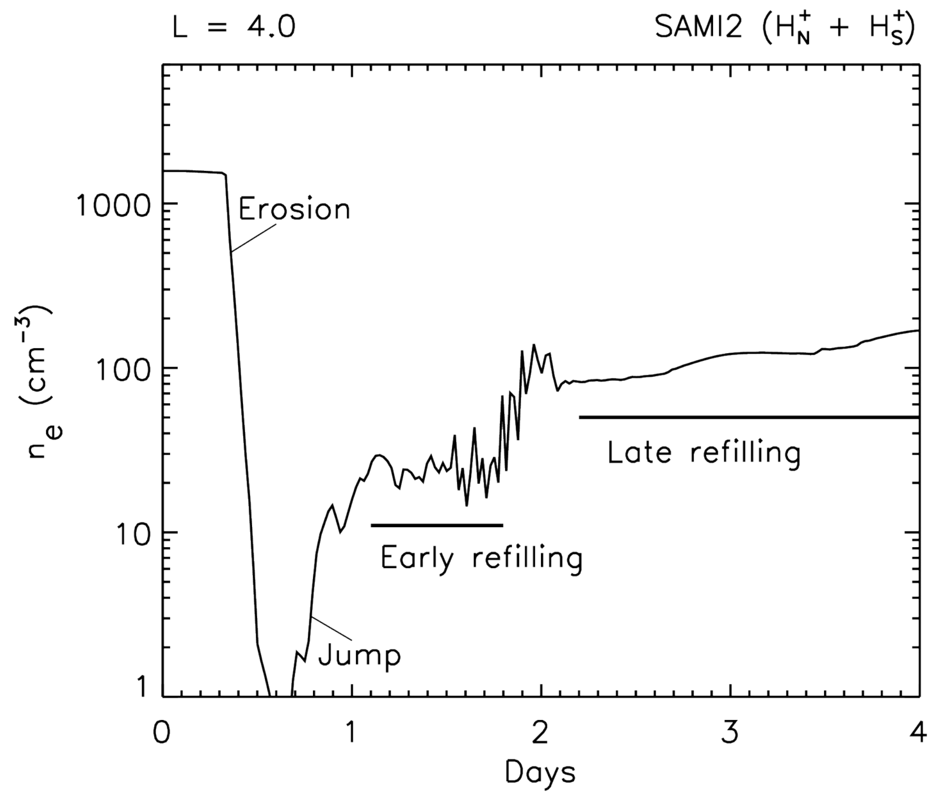

0. An initial jump, when the two outflow streams cross [Liemohn et al., JGR, 1999]
1. Early stage refilling, when H+ ions are counter-streaming.
2. Late stage refilling, when a single-fluid description is valid.

Plasmasphere refilling dynamics: numerical simulations

[Singh and Hwang, JGR, 1987]

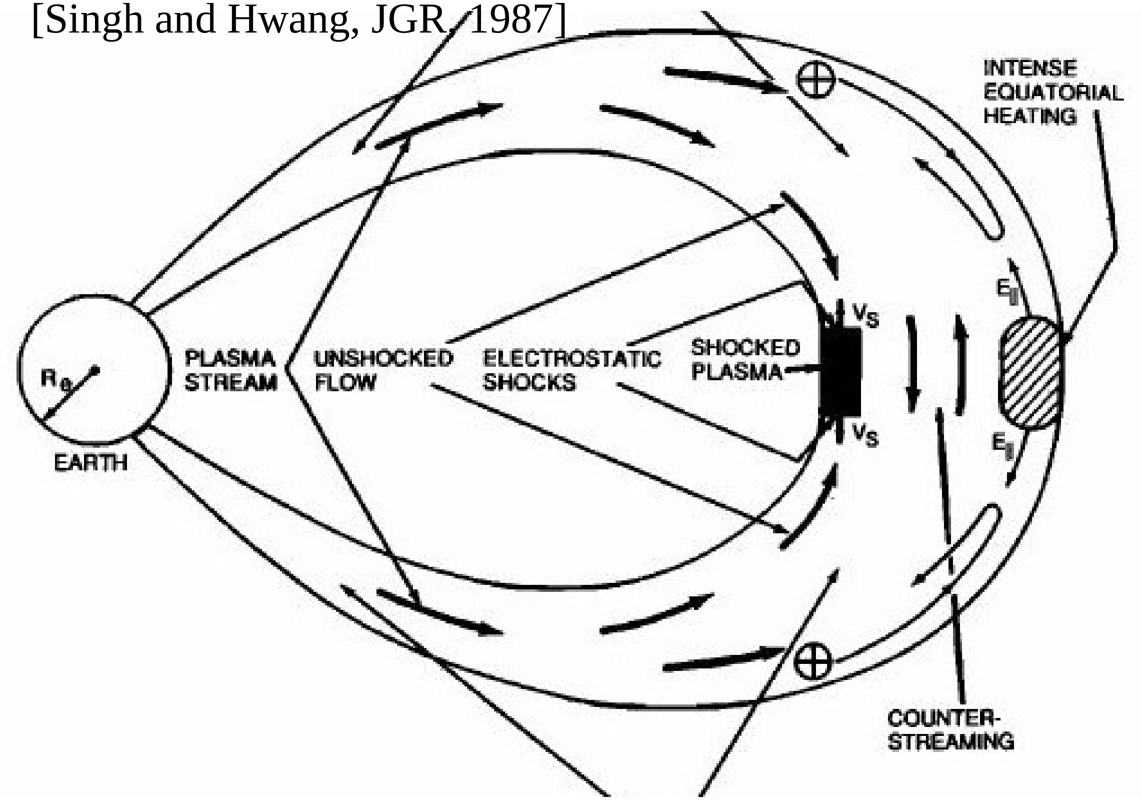

Initial modeling included only a single field-line, artificially low-density initial conditions and, usually, only H^+ outflow.

One-fluid models found colliding outflows and shocks.

With a single fluid description of H^+, northward and southward refilling outflows cannot pass through each other.

Plasmasphere refilling: counterstreaming H^+ outflows

[Singh and Horwitz, JGR, 1992]

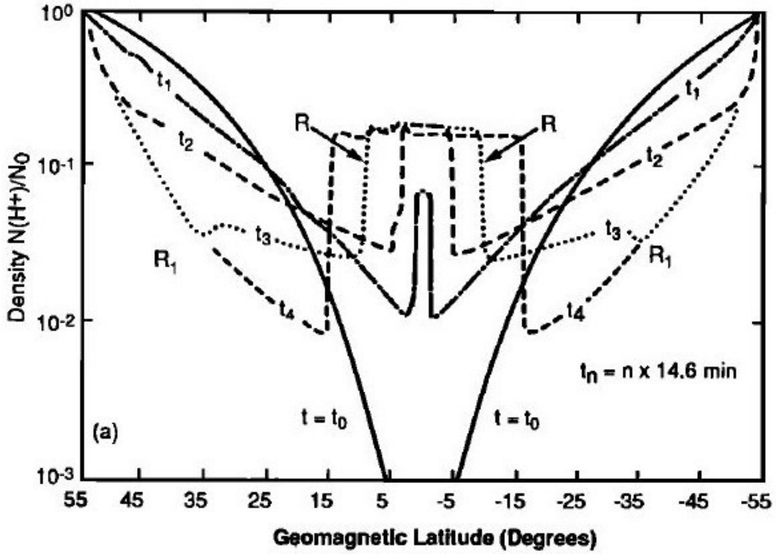

[Guiter et al., JGR, 1995]

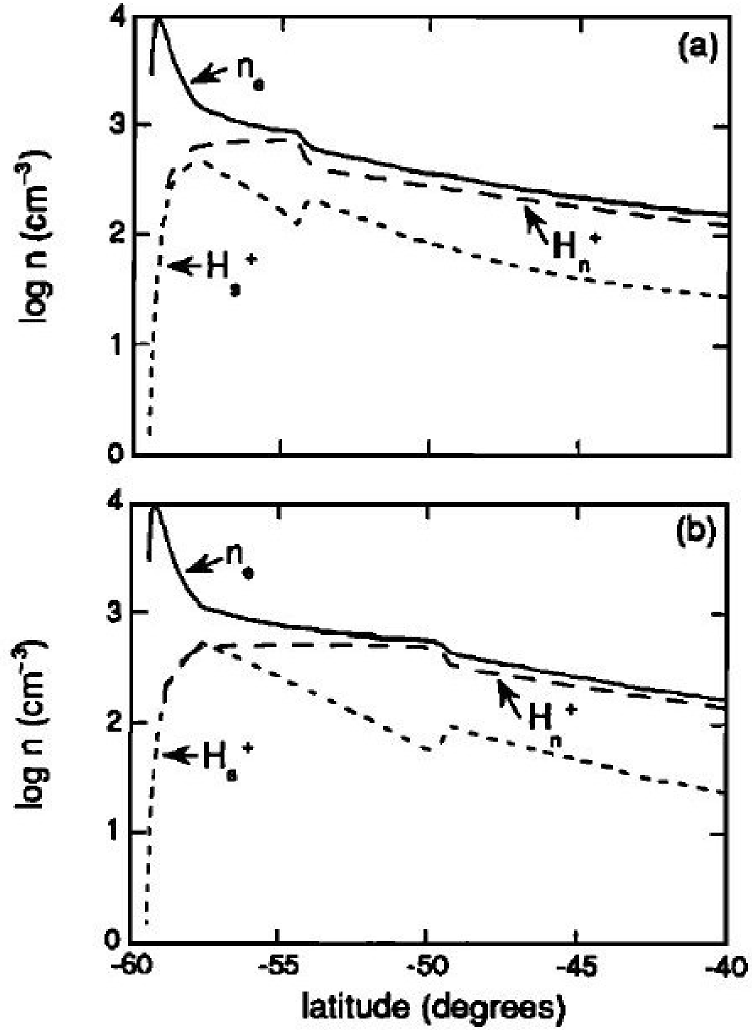

A one-fluid model has a shock at high altitude (“top-down” refilling).

A two-fluid model has two shocks at low altitude (“bottom-up” refilling).

Plasmasphere refilling: kinetic model of outflow

Kinetic simulation [Singh et al., JGR, 1994]

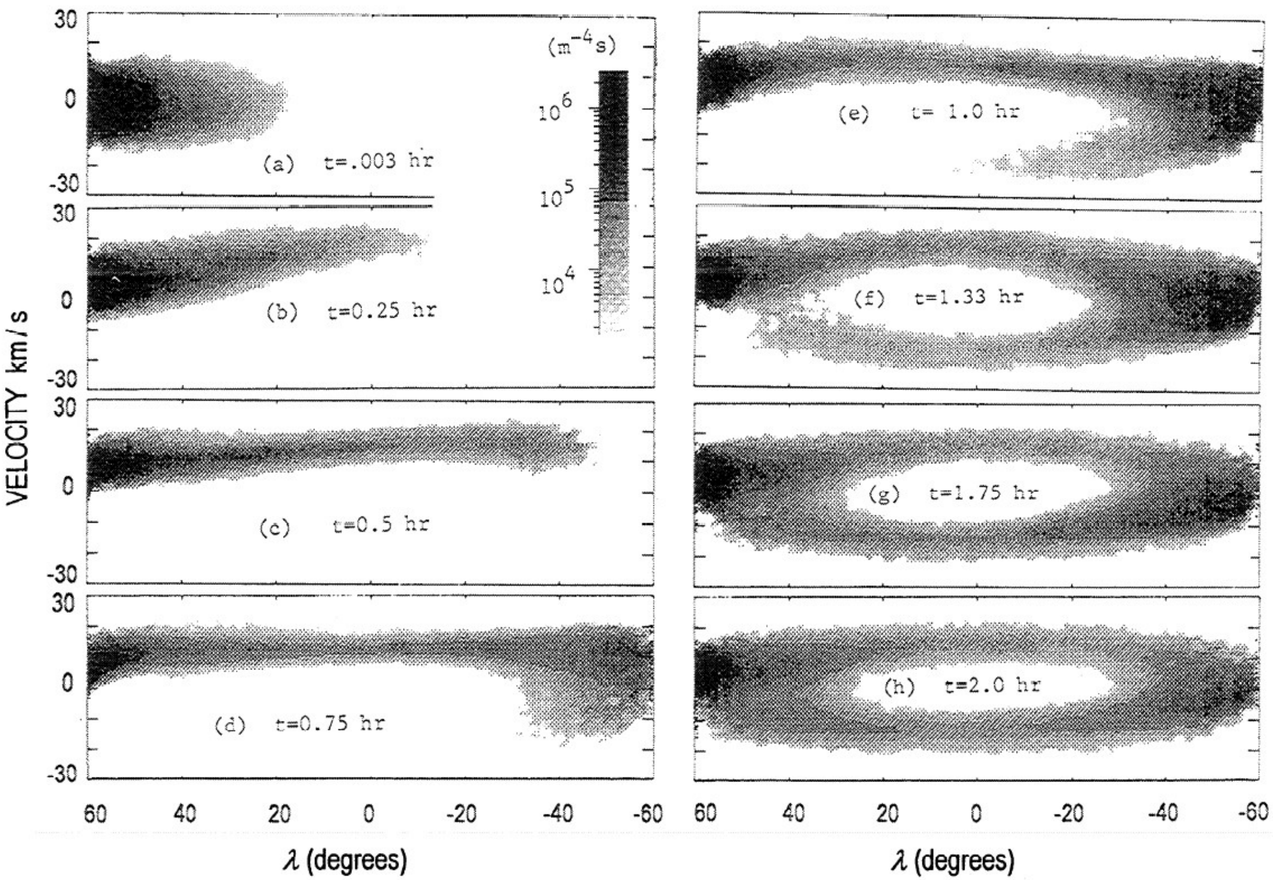

Figure 2. Temporal evolution of the flow originating from the northern hemisphere; phase-space ($s - V_{\parallel}$) plots are shown. The plot at t = .003 hour nearly shows the initial plasma in the flux tube.

The graphic shows only the outflow from the northern hemisphere.

Kinetic models find results similar to two-fluid results, with two shocks at low altitude.

Plasmasphere refilling dynamics: two-fluid H^+ model

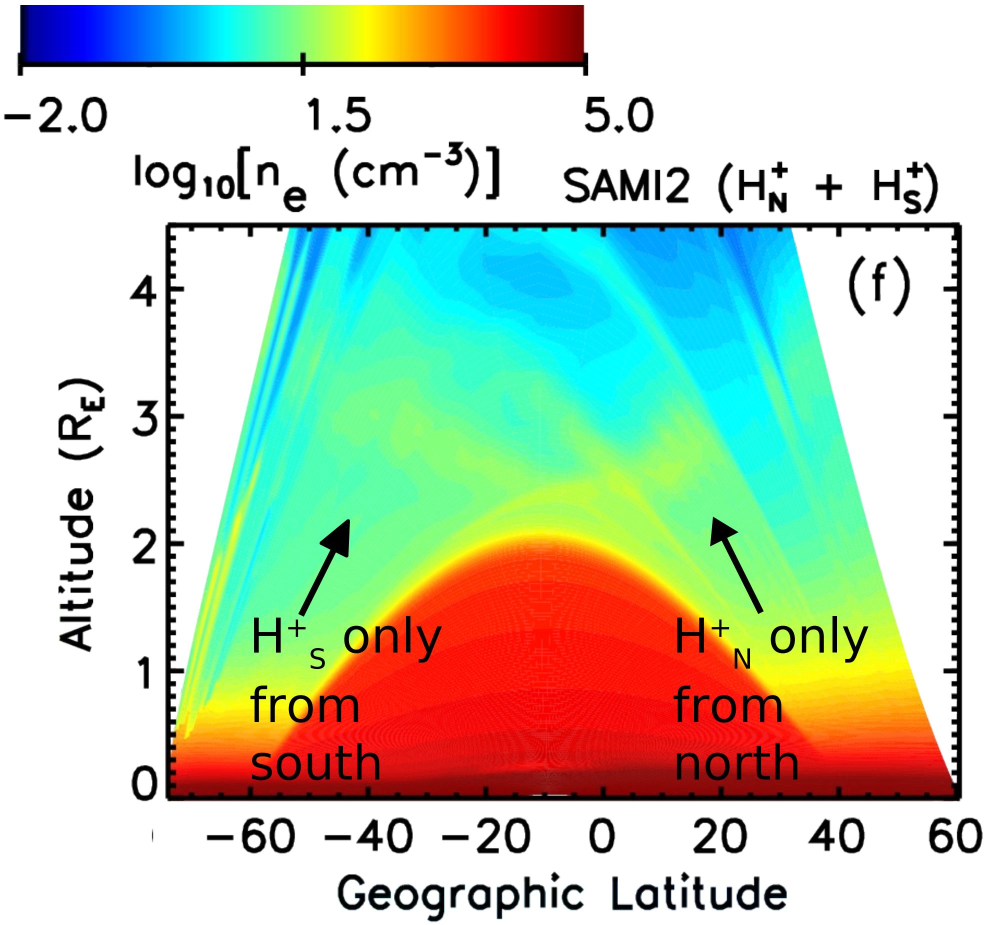

Updated SAMI2 has 8 ions instead of 7.

H^+ is replaced by:

- H^+_N created in the north
- H^+_S created in the south

[Krall & Huba, GRL, 2019]

Plasmasphere refilling dynamics: two-fluid H^+ model

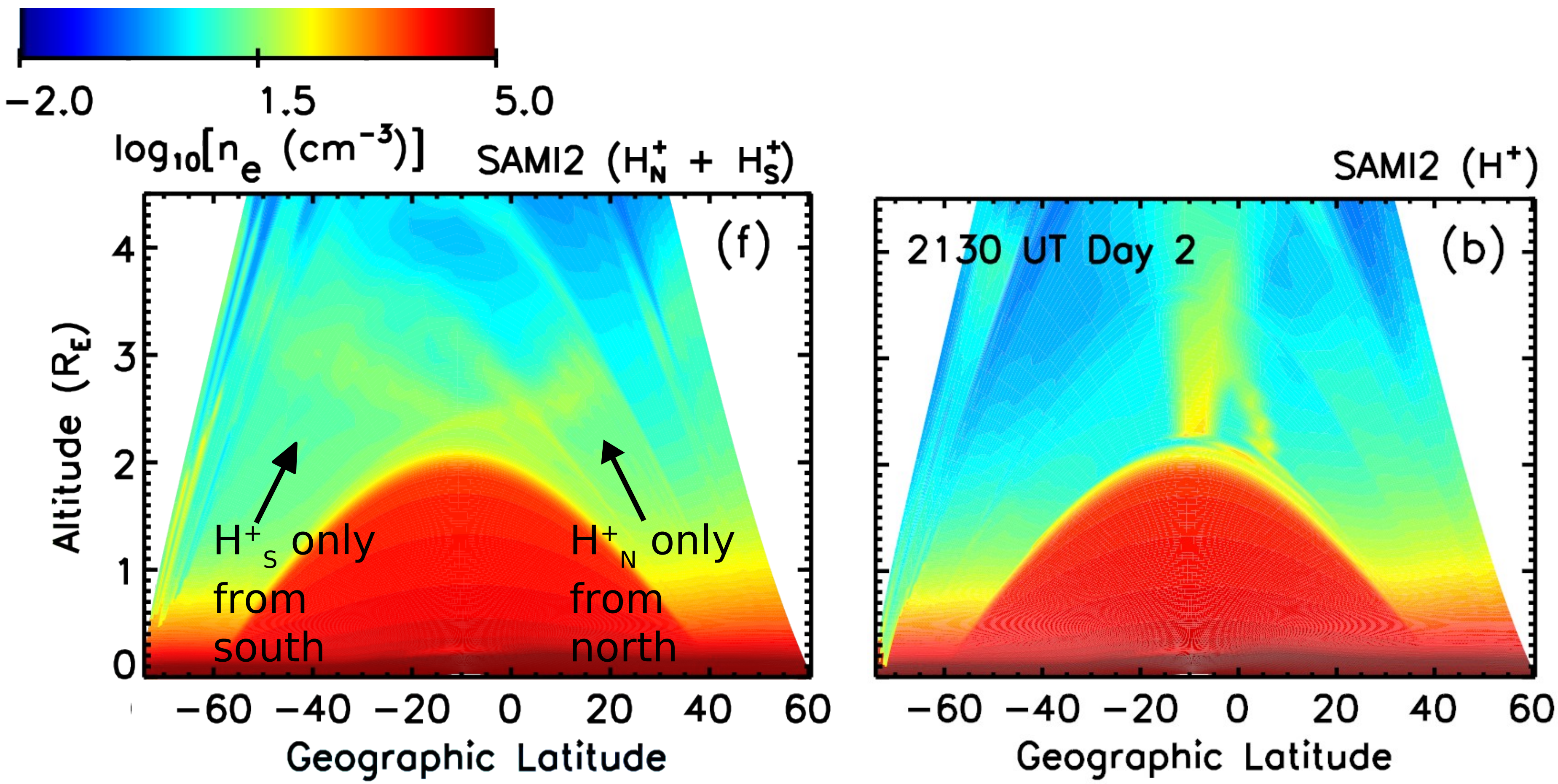

Plasmasphere refilling: “Top down” versus “bottom up”

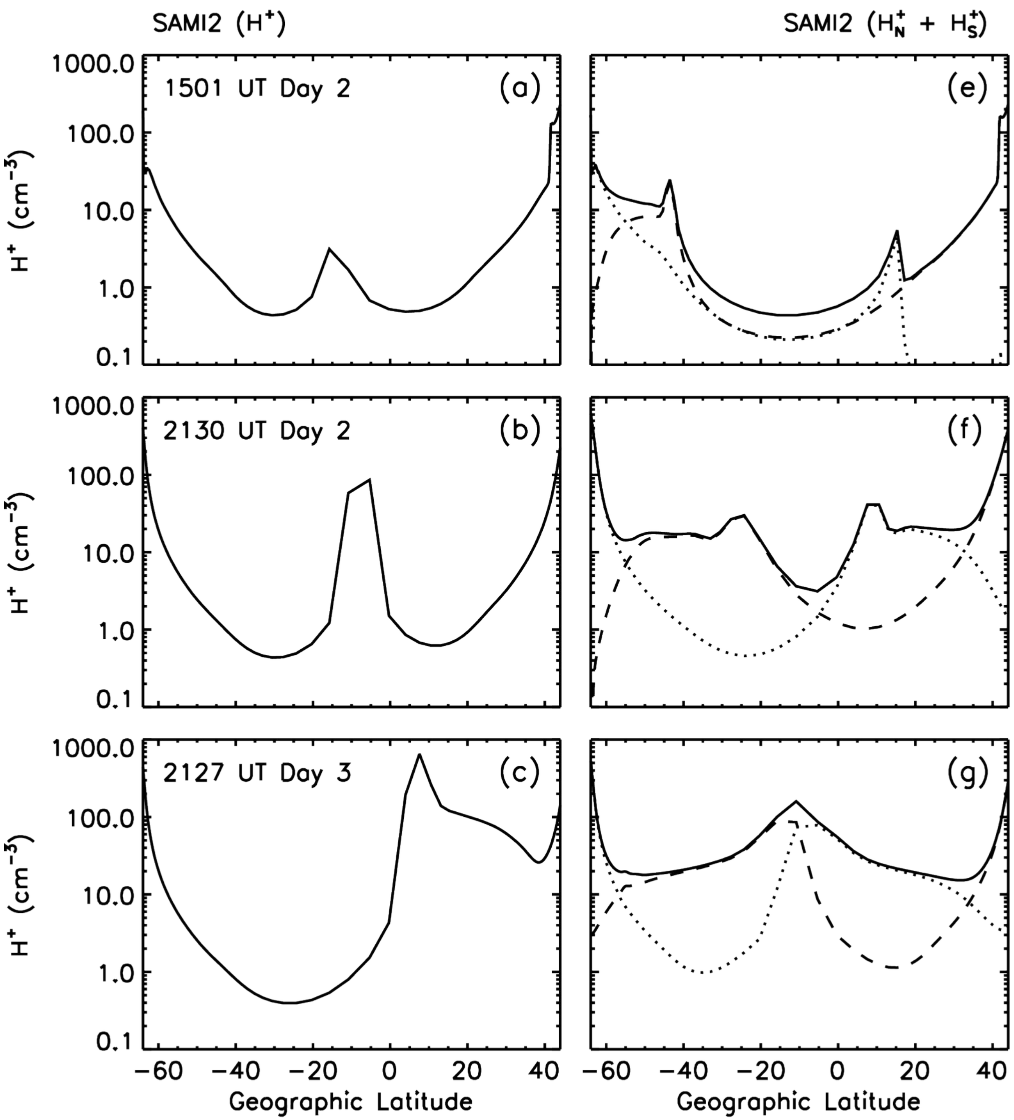

SAMI2 is used to simulate refilling using two H^+ species, one with a source only in the north and one with a source only in the south.

The two-fluid H^+ model and the the usual one-fluid H^+ model produce identical results in the ionosphere.

Plasmasphere refilling dynamics: early-stage and late-stage

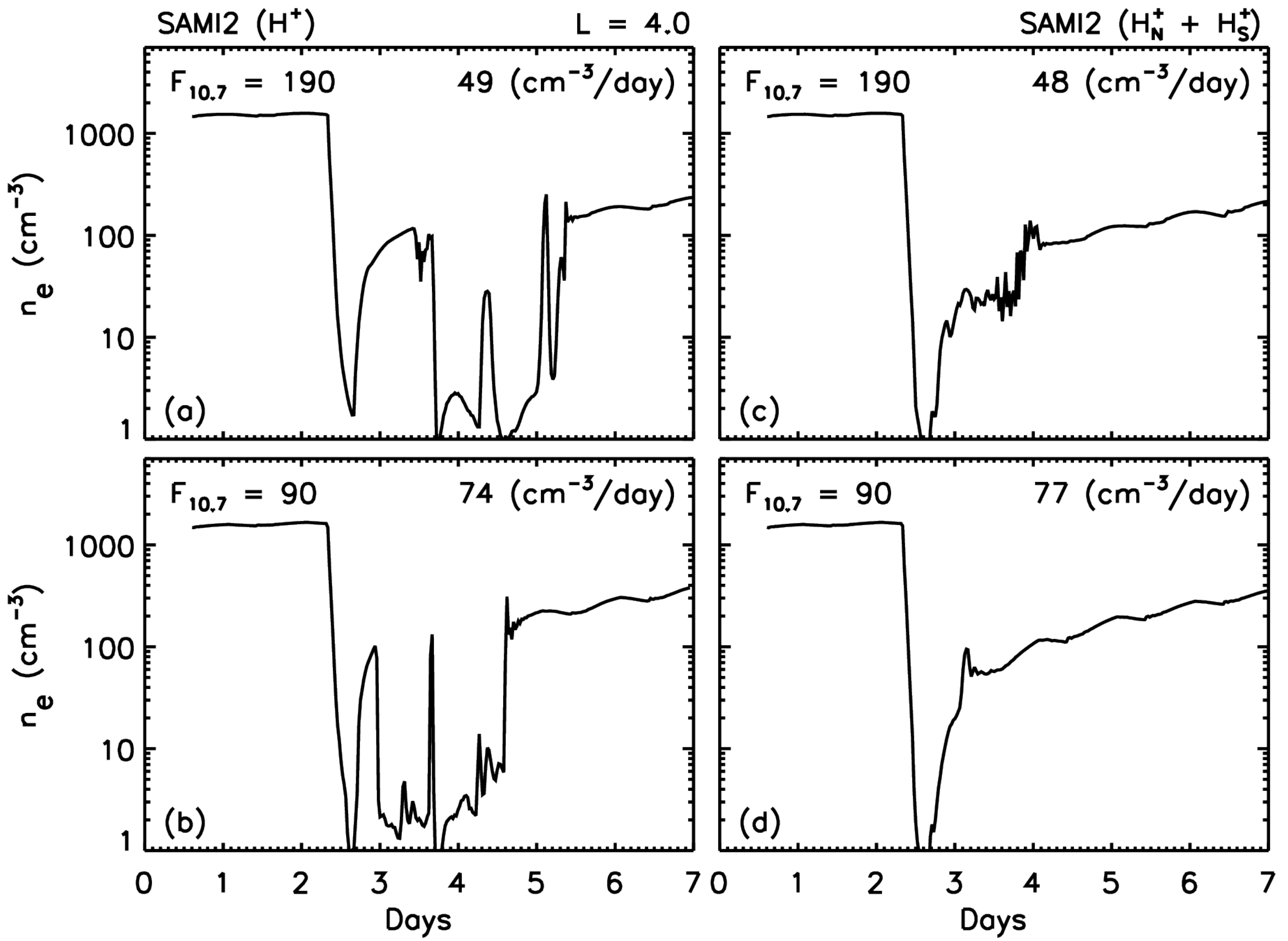

Single-fluid models can describe late-stage refilling.

SAMI3 with 2-fluid H^+

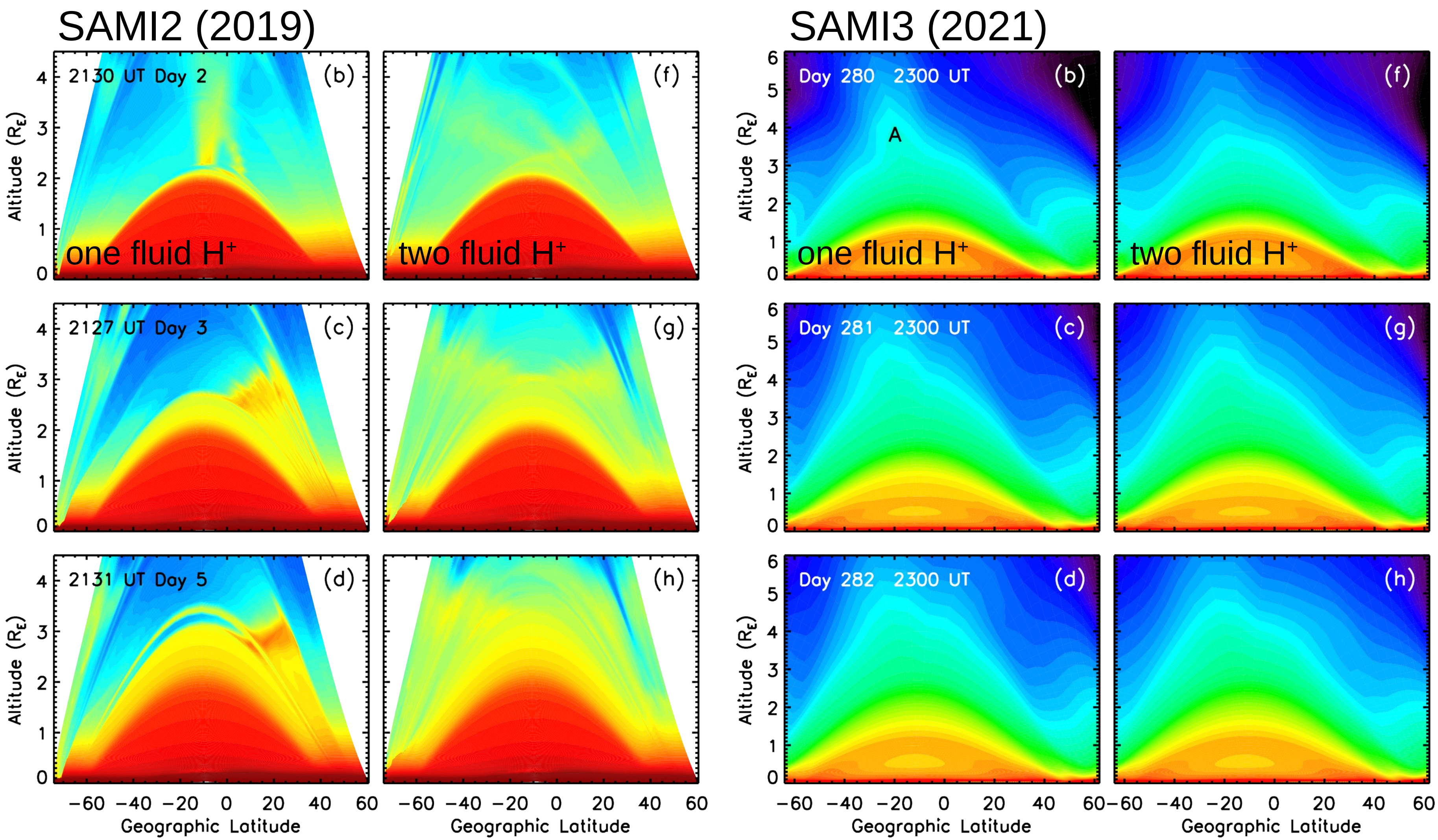

[Krall & Huba, FASS, 2021]

SAMI3 with 2-fluid H^+

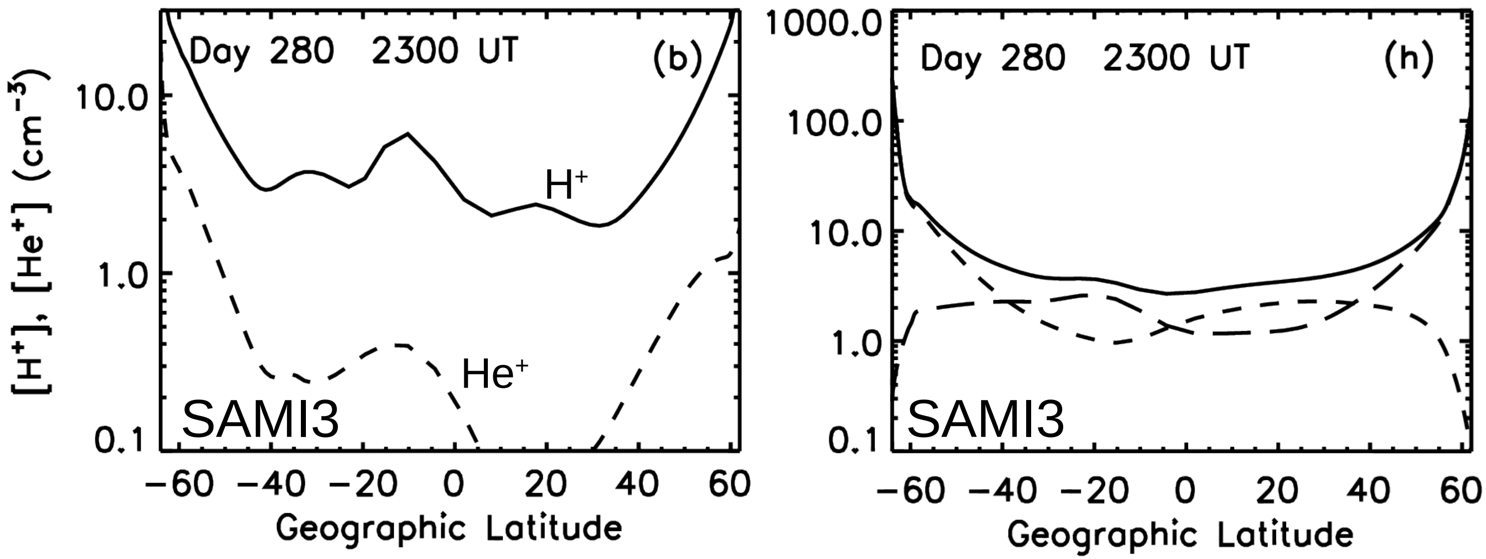

Without the artificial initial conditions of the older 1D and 2D (SAMI2) runs, SAMI3 produces a weak top-down refilling peak.

While the two-stream H^+ model *is* needed for studies of early stage refilling, it is otherwise not all that impactful.

References

Bishop, J. (1991), Analytic exosphere models for geocoronal applications, Planetary and Space Science, 39, 885-893, doi:10.1016/0032-0633(91)90093-P

Borovsky, J. E., Welling, D. T., Thomsen, M. F., and Denton, M. H. (2014), Long-lived plasmaspheric drainage plumes: Where does the plasma come from?, J. Geophys. Res. Space Physics, 119, 6496– 6520, doi:10.1002/2014JA020228

Denton, R. E., Wang, Y., Webb, P. A., Tengdin, P. M., Goldstein, J., Redfern, J. A., and Reinisch, B. W. (2012), Magnetospheric electron density long-term (>1 day) refilling rates inferred from passive radio emissions measured by IMAGE RPI during geomagnetically quiet times, J. Geophys. Res., 117, A03221, doi:10.1029/2011JA017274.

Foster, J. C., P. J. Erickson, A. J. Coster, J. Goldstein, and F. J. Rich (2002), Ionospheric signatures of plasmaspheric tails, Geophys. Res. Lett., 29(13), 10.1029/2002GL015067

Guiter, S. M., Gombosi, T. I., and Rasmussen, C. E. (1995), Two-stream modeling of plasmaspheric refilling, J. Geophys. Res., 100(A6), 9519– 9526, doi:10.1029/95JA00081

Huba, J. D., Joyce, G., and Fedder, J. A. (2000), Sami2 is Another Model of the Ionosphere (SAMI2): A new low-latitude ionosphere model, J. Geophys. Res., 105(A10), 23035-23053, doi:10.1029/2000JA000035

Huba, J. D., and J. Krall (2013), Modeling the plasmasphere with SAMI3, Geophys. Res. Lett., 40, 6-10, doi:10.1029/2012GL054300

Huba, J.D. and Joyce, G. (2014), Numerical Methods in Modeling the Ionosphere, in Modeling the Ionosphere–Thermosphere System (eds J. Huba, R. Schunk and G. Khazanov), doi:10.1002/9781118704417.ch5

References

Huba, J. D., Sazykin, S., and Coster, A. (2017), SAMI3-RCM simulation of the 17 March 2015 geomagnetic storm, J. Geophys. Res. Space Physics, 122, 1246-1257, doi:10.1002/2016JA023341

Ilie, Raluca, Ruth M. Skoug, Herbert O. Funsten, Michael W. Liemohn, J. J. Bailey and Mike Gruntman (2013). “The impact of geocoronal density on ring current development.” Journal of Atmospheric and Solar-Terrestrial Physics 99, 92-103, doi:10.1016/j.jastp.2012.03.010

Krall, J., Huba, J. D., & Borovsky, J. E. (2018). SAMI3 simulations of a persistent plasmasphere plume. Geophysical Research Letters, 45, 3374-3381. https://doi.org/10.1002/2017GL076448

Krall, J., Glocer, A., Fok, M.-C., Nossal, S. M., & Huba, J. D. (2018). The unknown hydrogen exosphere: Space weather implications. Space Weather, 16, 205– 215. https://doi.org/10.1002/2017SW001780

Krall, J., & Huba, J. (2019), Simulation of counterstreaming H+ outflows during plasmasphere refilling, Geophysical Research Letters, 46, 3052-3060, doi:10.1029/2019GL082130

Krall J. and Huba J. D. (2021), Counterstreaming Cold H+, He+, O+, and N+ Outflows in the Plasmasphere. Front. Astron. Space Sci., 8:712611, doi: 10.3389/fspas.2021.712611

Lawrence, D. J., Thomsen, M. F., Borovsky, J. E., and McComas, D. J. (1999), Measurements of early and late time plasmasphere refilling as observed from geosynchronous orbit, J. Geophys. Res., 104(A7), 14691-14704, doi:10.1029/1998JA900087

Liemohn, M. W., Khazanov, G. V., Craven, P. D., and Kozyra, J. U. (1999), Nonlinear kinetic modeling of early stage plasmaspheric refilling, J. Geophys. Res., 104(A5), 10295-10306, doi:10.1029/1999JA900104

References

Obana, Y., F. W. Menk, and I. Yoshikawa (2010), Plasma refilling rates for L = 2.3–3.8 flux tubes, J. Geophys. Res., 115, A03204, doi:10.1029/2009JA014191

Rasmussen, C. E., S. M. Guiter, and S. G. Thomas (1993), Two-dimensional model of the plasmasphere: refilling time constants, Planet. Space Sci., 41, 35-43, doi:10.1016/0032-0633(93)90015-T

Reinisch, B.W., M.B. Moldwin, R.E. Denton, D.L. Gallagher, H. Matsui, V. Pierrard, J. Tu (2009), Augmented empirical models of plasmaspheric density and electric field using IMAGE and CLUSTER data, Space Sci Rev, 145: 231-261, DOI 10.1007/s11214-008-9481-6

Shi, Q., Zong, QG., Fu, S. et al. (2013), Solar wind entry into the high-latitude terrestrial magnetosphere during geomagnetically quiet times, Nat Commun 4, 1466, doi:10.1038/ncomms2476

Singh, N. and Hwang, K.S. (1987). Perpendicular ion heating effects on the refilling of the outer plasmasphere. Journal of Geophysical Research 92: doi: 10.1029/JA080i012p13513. Issn: 0148-0227

Singh, N., and Horwitz, J. L. (1992), Plasmasphere refilling: Recent observations and modeling, J. Geophys. Res., 97(A2), 1049-1079, doi:10.1029/91JA02602

Singh, N., Wilson, G. R., and Horwitz, J. L. (1994), Comparison of hydrodynamic and semikinetic treatments for a plasma flow along closed field lines, J. Geophys. Res., 99(A6), 11495-11506, doi:10.1029/93JA03027

Thomas, E. G., Baker, J. B. H., Ruohoniemi, J. M., Clausen, L. B. N., Coster, A. J., Foster, J. C., and Erickson, P. J. (2013), Direct observations of the role of convection electric field in the formation of a polar tongue of ionization from storm enhanced density, J. Geophys. Res. Space Physics, 118, 1180–1189, doi:10.1002/jgra.50116

Extra: Plume dynamics

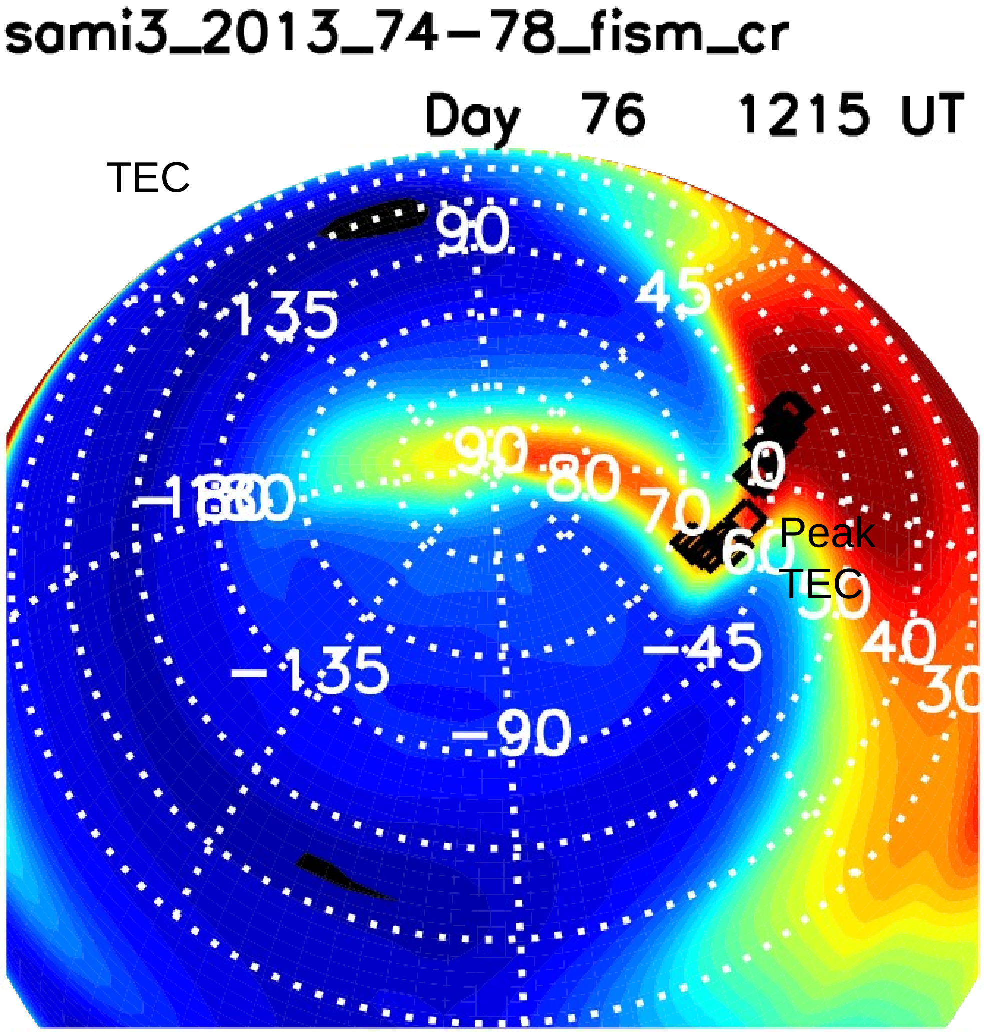

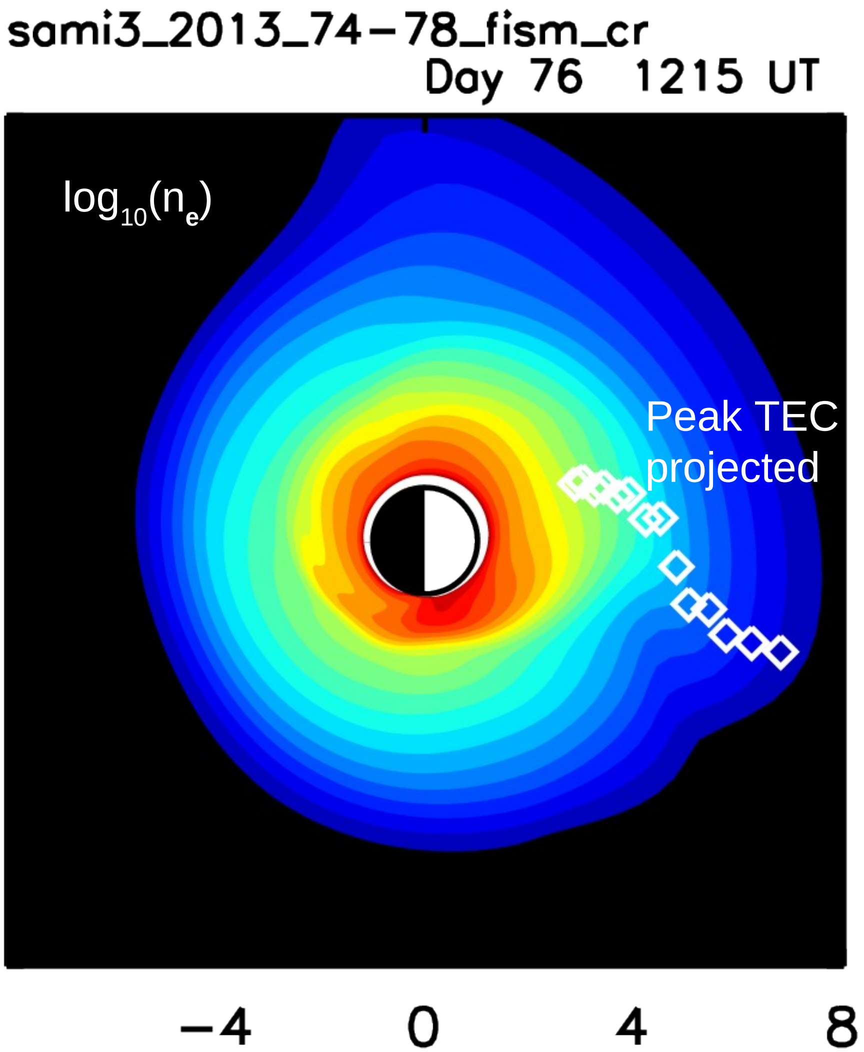

In what ways is the plume coupled to the ionosphere?

Subauroral Polarization Stream (SAPS)

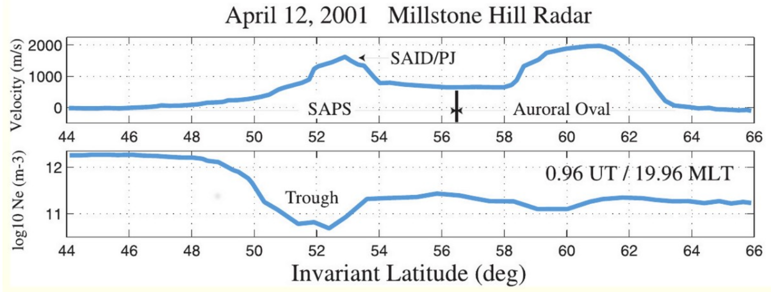

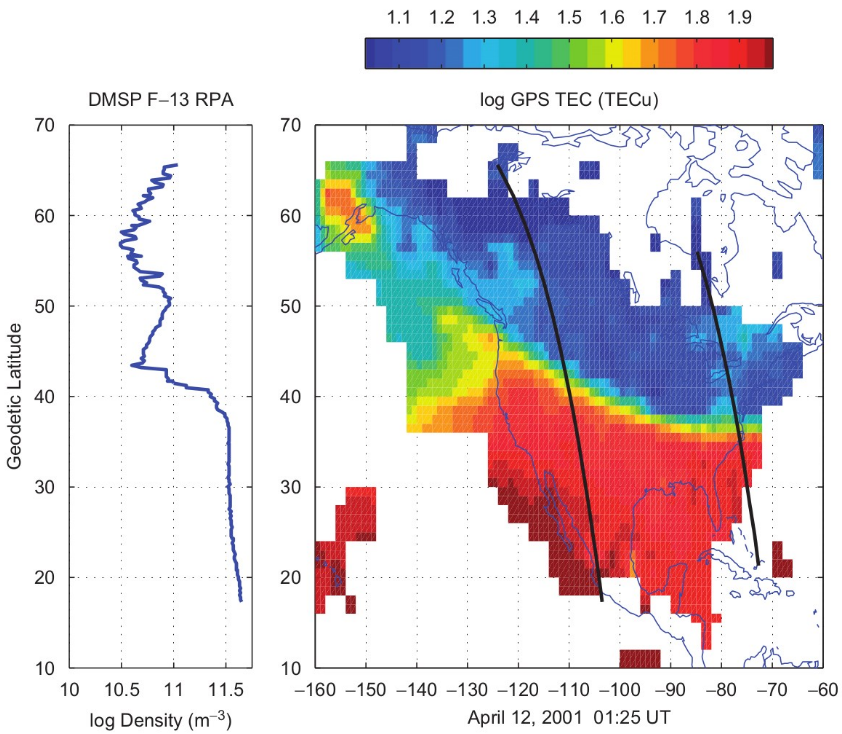

SAPS is a strong westward and poleward drift associated with the low-density trough. Observations suggest that SAPS can affect the storm-enhanced density (SED), drawing plasma westward an poleward.

The proximity of low density SAPS to the high-density SED creates a strong density gradient.

[Foster and Vo, JGR, 2003; Foster et al., JASTP, 2007]

Example: SAMI3/RCM modeling of storms

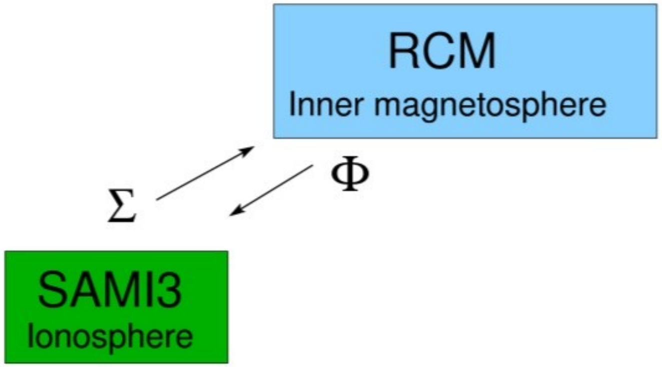

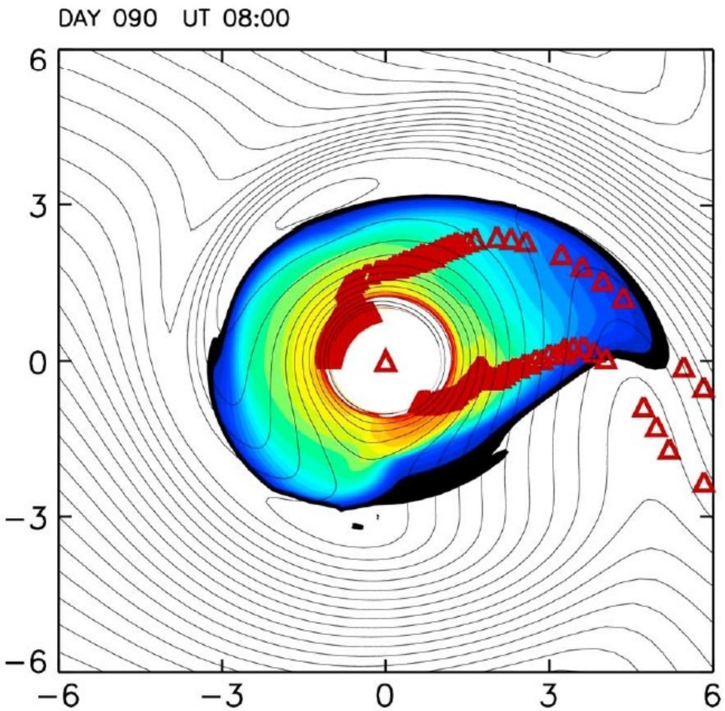

HENA(FUV), EUV image (J. Goldstein)

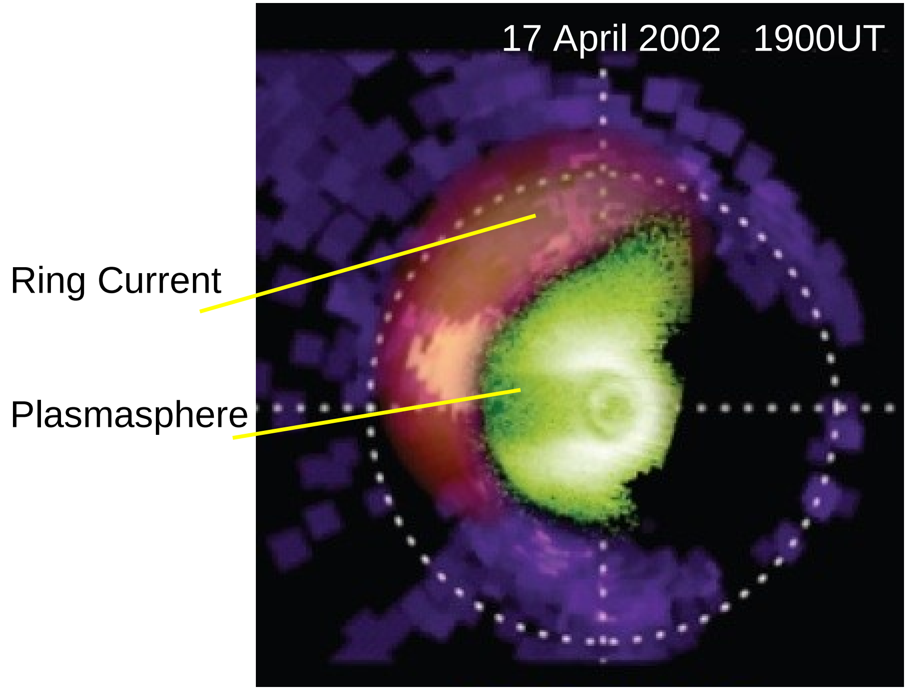

[Huba and Sazykin, GRL, 2014; see also Huba et al., GRL, 2005]

SAPS and TOI features

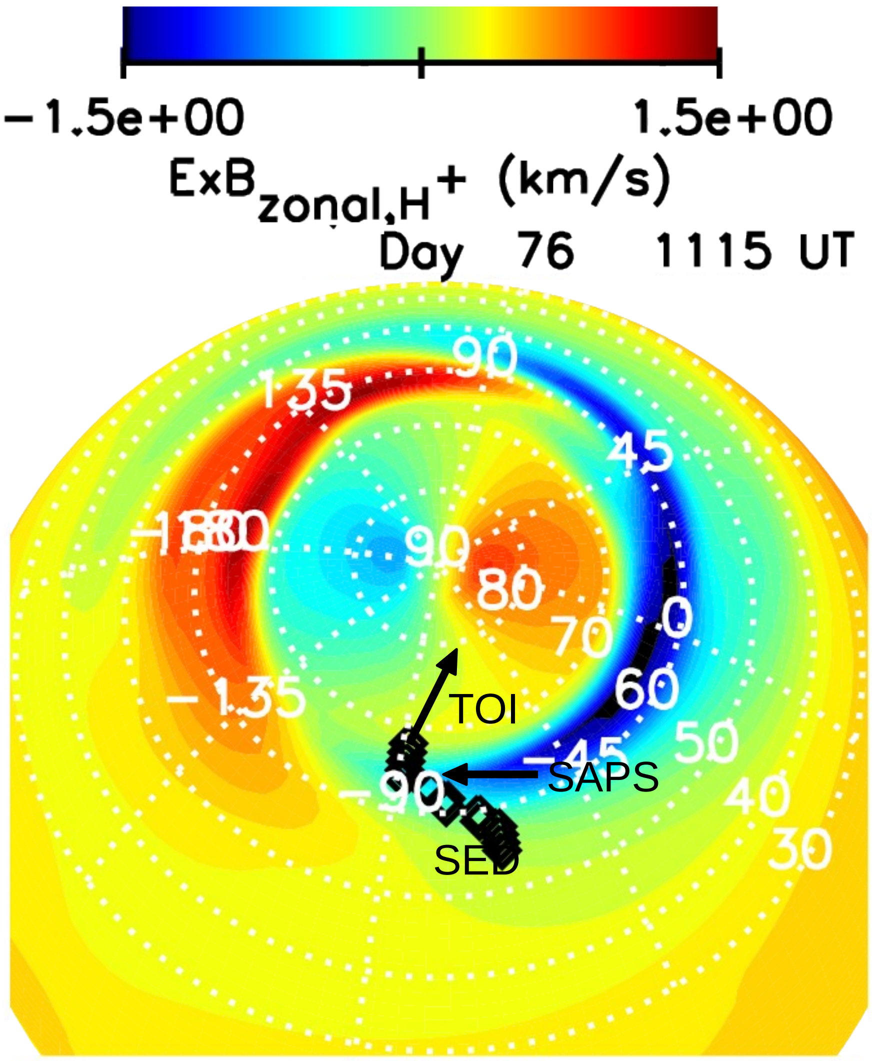

The zonal drift is plotted for a SAMI3/GITM/RCM run.

The westward (dawnward) SAPS field is the strong negative zonal drift (blue/black).

SAPS is a strongest in the pre-midnight sector, where it contributes to the erosion of the plasmasphere.

The peak in TEC is marked at each latitude with a symbol.

Does SAPS affect plume dynamics?

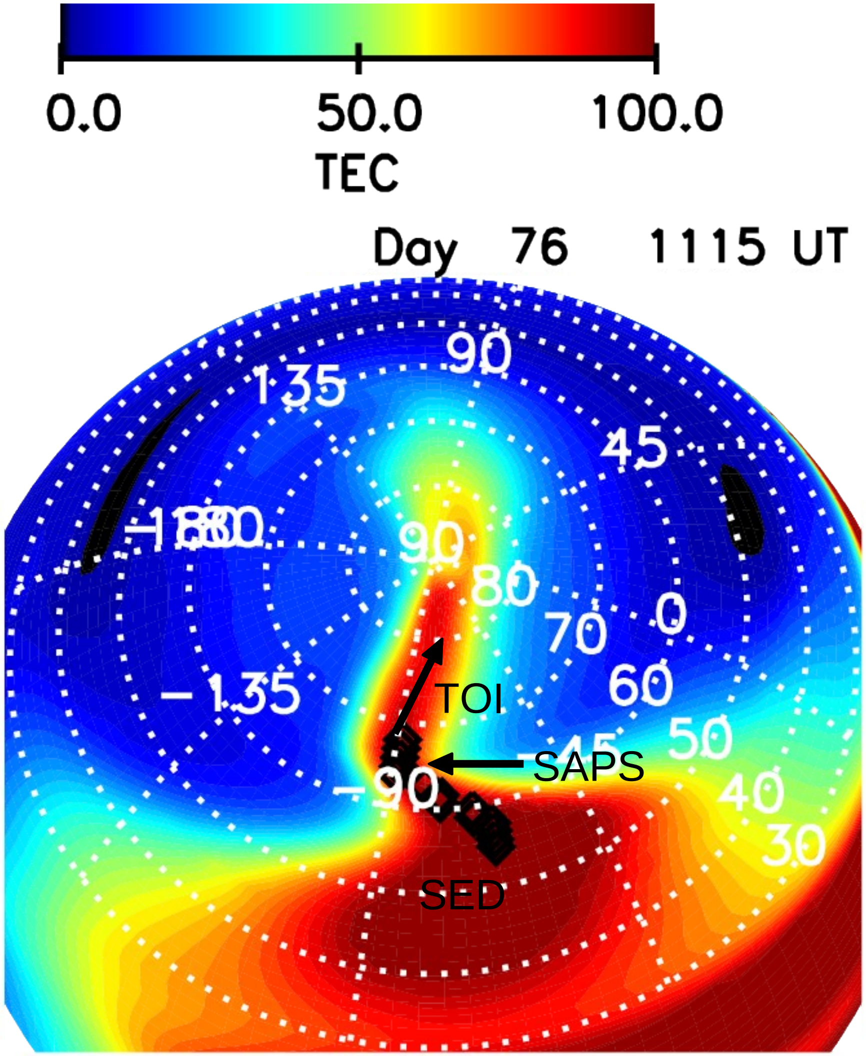

We will look for cases where the SAPS feature is strong, as indicated by enhanced density and a long dawnward deflection of the poleward **E** x **B** drift.

Question: Does a strong SAPS feature correlate with a change in the position of the plasmasphere plume?

SAPS and plume dynamics: 4 storms

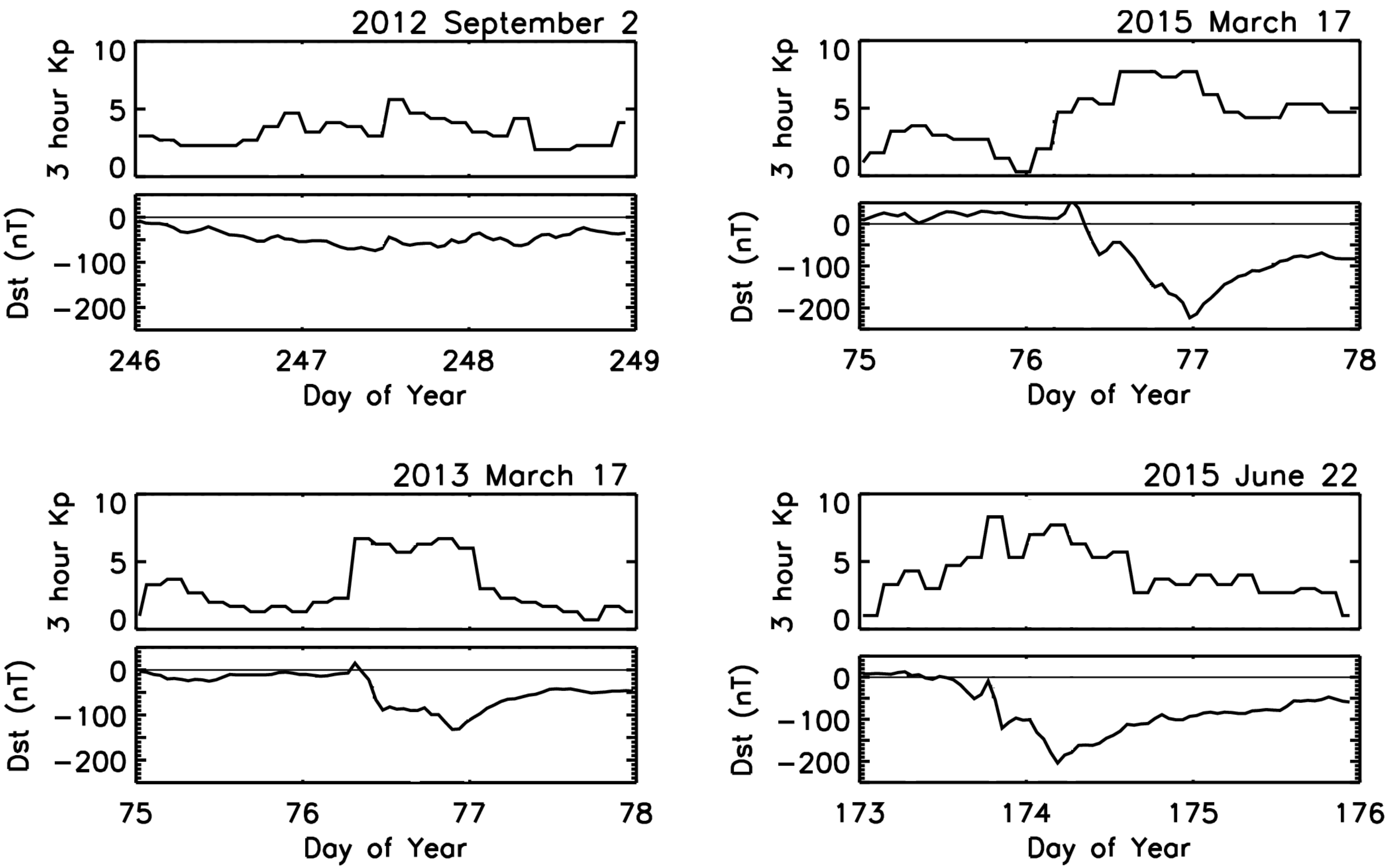

SAPS and plume dynamics: 2012 09 03 storm

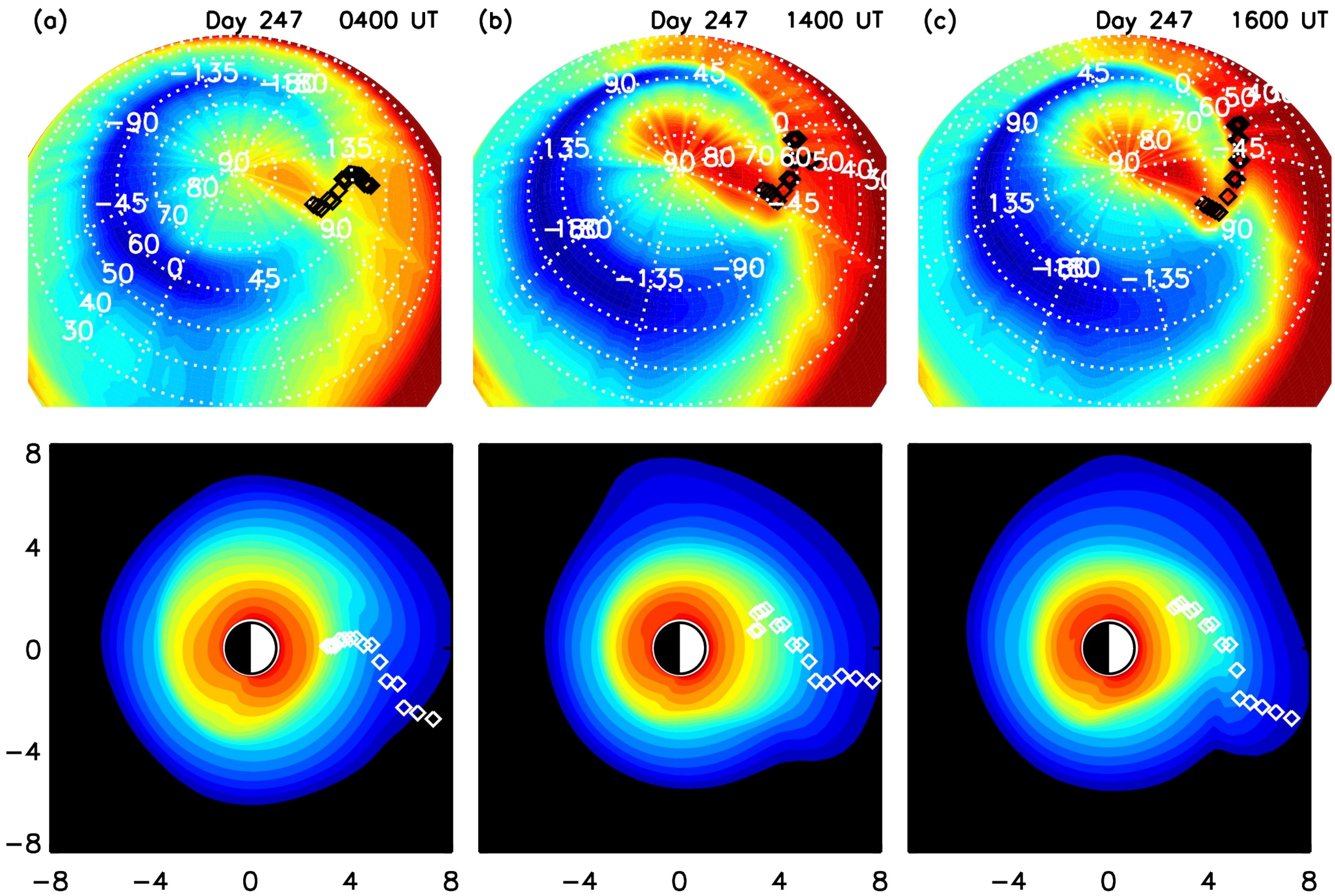

SAPS and plume dynamics: 2013 03 17 storm

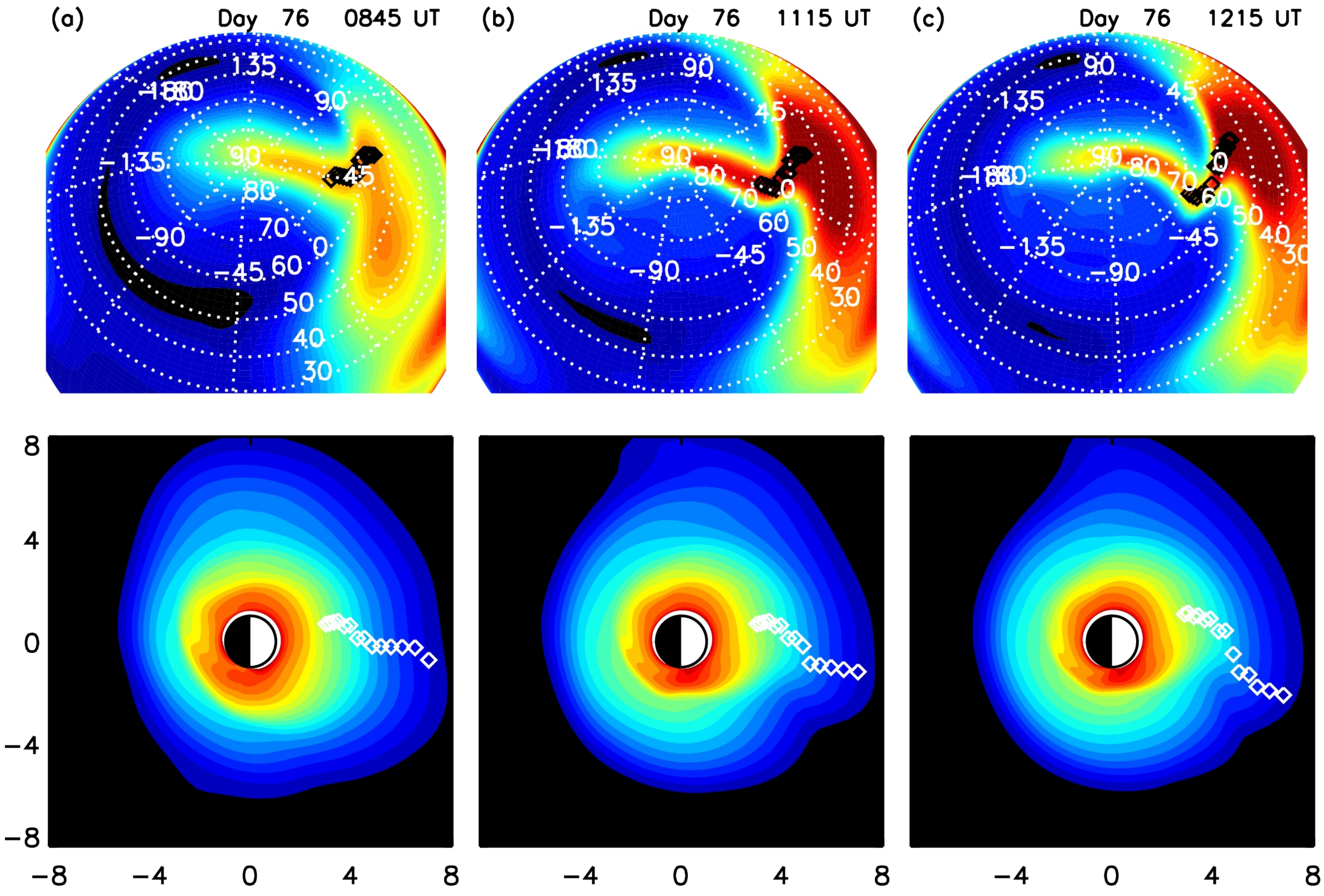

SAPS and plume dynamics: 2015 03 17 storm

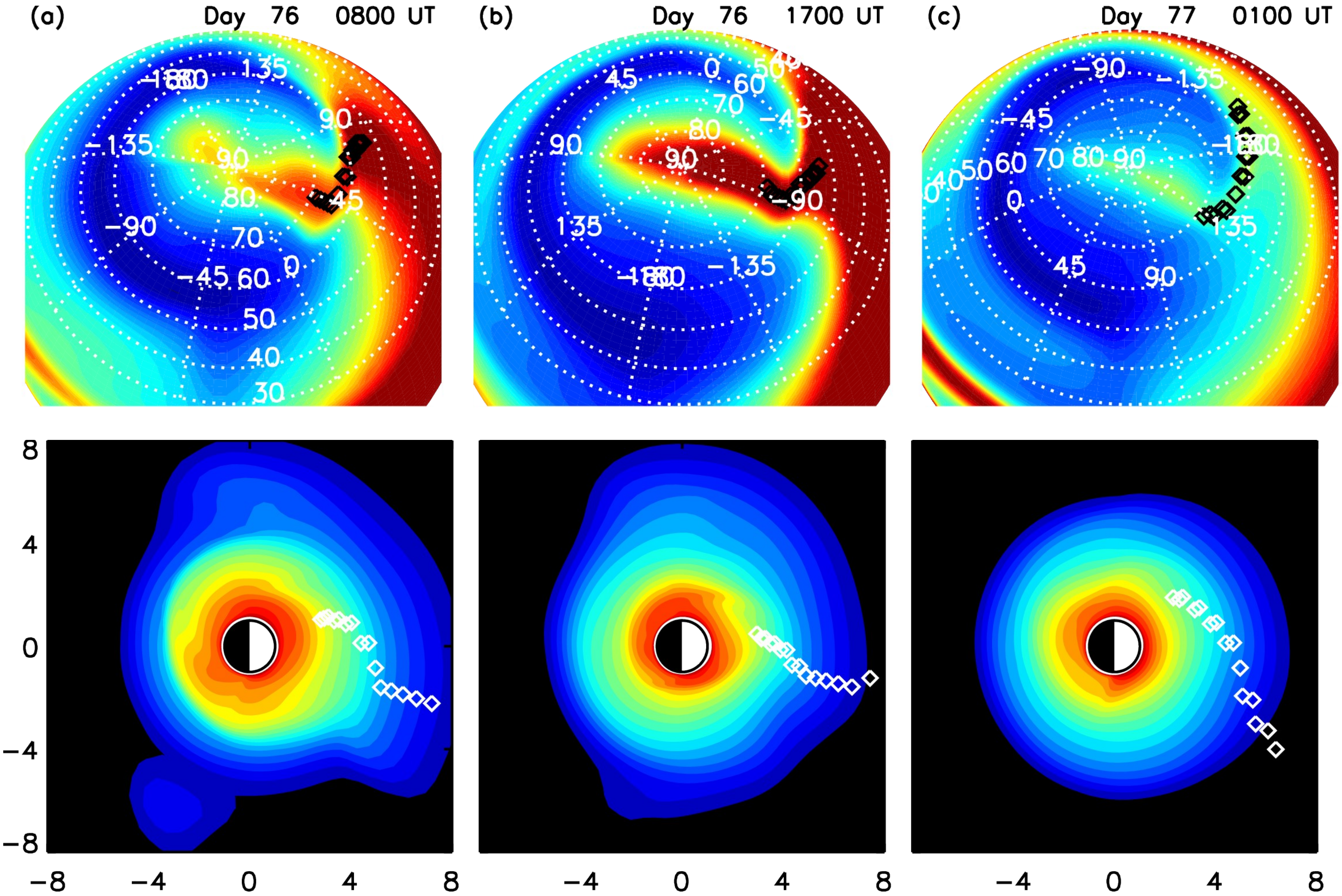

SAPS and plume dynamics: 2015 06 22 storm

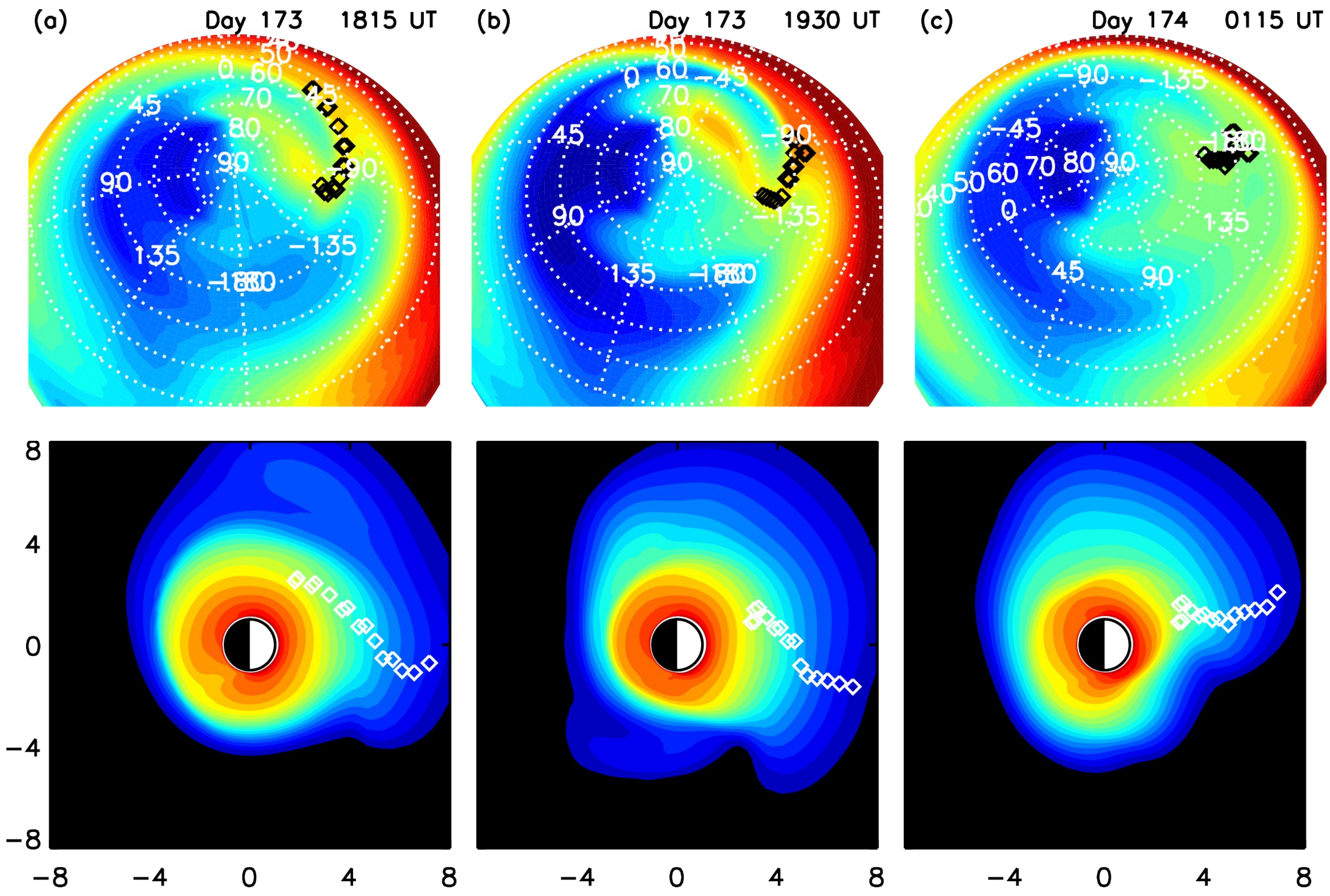

Does SAPS affect plume dynamics?

The SAPS **E** field appears to deflect the plume towards dawn.

As the storm abates, the correlation seems to weaken, as in the 2015, day 77, 0100 UT case.

Does the plume co-rotate with the plasmasphere?

How well-correlated are TOI and plume densities?

How do plasma and convection time scales (minimizes to hours) shape the plume?

Note: in some runs we use SAMI3/RCM

More references

Foster, J. C., and H. B. Vo (2003), Average characteristics and activity dependence of the subauroral polarization stream, J. Geophys. Res., 107(A12), 1475, doi:10.1029/2002JA009409.

Foster, J. C., W. Rideout, B. Sandel, W.T. Forrester, F.J. Rich (2007), On the relationship of SAPS to storm-enhanced density, Journal of Atmospheric and Solar-Terrestrial Physics, 69, 303-313, doi:10.1016/j.jastp.2006.07.021.

Huba, J. D., G. Joyce, S. Sazykin, R. Wolf, and R. Spiro (2005), Simulation study of penetration electric field effects on the low- to mid-latitude ionosphere, Geophys. Res. Lett., 32, L23101, doi:10.1029/2005GL024162

Huba, J. D., and S. Sazykin (2014), Storm time ionosphere and plasmasphere structuring: SAMI3-RCM simulation of the 31 March 2001 geomagnetic storm, Geophys. Res. Lett., 41, 8208– 8214, doi:10.1002/2014GL062110.